K_2CO_3-Li_2CO_3 Molten Carbonate Mixtures and Their Nanofluids for Thermal Energy Storage: An Overview of the Literature

Navarrete, N.[1], Nithiyanantham, U. [1,2], Hernández, L.[1], Mondragón, R.[1,*]

[1] Departamento de Ingeniería Mecánica y Construcción, Universitat Jaume I, 12071-Castellón de la Plana, Spain

[2] Heat Transfer and Thermal Power Laboratory, Department of Mechanical Engineering, Indian Institute of Technology Madras, Chennai 600036, India.

Corresponding author: mondragn@uji.es

Abstract

The research and development of new thermal energy storage materials with high working temperatures are key topics to increase the efficiency of thermal energy to electricity conversion. The use of molten salt combinations with a wide range of operating temperatures is one of the ways to fulfil this purpose, and among them, molten carbonates present several advantages, such as high thermal stability, moderate cost, and less corrosiveness, compared to other molten salt mixtures. The present work contains a state-of-the-art review of the most important thermophysical properties for the thermal energy storage capacity of binary mixtures of potassium and lithium carbonates (K_2CO_3-Li_2CO_3). The available literature on the properties that play a key role in the heat transfer rate (viscosity and thermal conductivity) and volumetric storage capacity (melting point, density, latent heat of fusion and specific heat) is reviewed and presented. This includes the works that deal with nanofluids based on these binary mixtures of molten carbonates by analysing the influence of nanoparticles on thermophysical properties. Special attention is paid to specific heat as abnormal increases are registered in molten salts when introducing nanoparticles. Although future research is necessary about the thermophysical properties enhancement of these materials, the advanced capacities they offer for high-temperature thermal energy storage are promising, and this work aims to compile the available data on them until the present day.

Keywords: Thermal energy storage, carbonate mixtures, nanofluids, thermophysical properties

Highlights

- Thermal energy storage through molten salts plays a key role in sustainable energy
- Carbonate mixtures are a promising alternative for high temperature thermal storage
- Thermophysical property data for K_2CO_3-Li_2CO_3 mixtures are discussed and reviewed
- Molten salt based nanofluids can present enhanced thermophysical properties
- Mechanisms involved in the nanofluids specific heat enhancement are discussed

Nomenclature

CSP	Concentrated solar power
CPCM	Composite phase change material
DSC	Differential scanning calorimetry
HTF	Heat transfer fluid
LCOE	Levelised Cost of Electricity
MDSC	Modulated differential scanning calorimetry
MWCNT	Multi-walled carbon nanotubes
PCM	Phase change material
SEM	Scanning electron microscopy
SWCNT	Single-walled carbon nanotubes
TES	Thermal energy storage

Symbols

α	Thermal diffusivity
c_p	Specific heat
$\Delta \mathrm{H}$	Phase change enthalpy
ΔT	Temperature step
η	Viscosity
E_η	Activation energy
k	Thermal conductivity
m	Mass
Q	Thermal energy stored
ρ	Density
R	Universal constant of gases
T	Temperature
V	Volume

Subscripts

$sensible$	Sensible heat
$latent$	Latent heat
m	Melting
max	Maximum
$mixture$	Multicomponent mixture

1. Introduction

One of the biggest challenges of our time is to reduce CO_2 and other greenhouse gas emissions in order to mitigate their effect on climate change and global warming [1]. One key point to fulfil this goal is the so-called energy transition: i.e., changing the current model of energy production based on fossil fuels to renewable and cleaner energy sources. However, a critical issue for this transition is the intermittency of some of these sources, namely solar, wind or wave power and hydropower, which can result in uneven power generation availability and mismatches between energy production and use periods. In order to evade these problems, the following are necessary: suitable energy storage capable of keeping power production plants running when the source is unavailable, or continue to meet usage needs even if no energy is being produced at a given time.

The mechanisms followed for this necessary energy storage vary and vastly differ according to the energy source. In solar thermal energy plants, commonly known as concentrated solar power (CSP) plants, the most common mechanism of energy storage consists in adding two tanks filled with molten salts (one hot, one cold) to the general circuit. Thus, when harvesting solar energy, the cold salt is heated by excess energy and is transferred to the hot tank. Whereas when sunlight is not available (due to weather conditions or at night-time), salts are moved from the hot tank to the cold one, passing through a heat exchanger that raises the temperature of the common heat transfer fluid (HTF) used to keep the installation working [2].

Several configurations of CSP plants are possible that depend on, among other factors, the maximum temperature that the fluid used for heat transfer can reach. In fact, certain configurations exist that employ molten salts directly, such as HTF and thermal energy storage material [3]. Accordingly, different materials are used for thermal energy storage depending on the temperatures reached and applications. Among them, solar salt, which consists of 42 mol% KNO_3 and 58 mol% $NaNO_3$, was the most commonly used material for commercial CSP applications [4]. However, the currently used nitrate based molten salts decompose at around 600 °C [5] and therefore, the upper operating temperature of the current TES system is limited to 560 °C due to the maximum working temperature of the molten salt [6]. If the operating temperature of the system was increased above 700 °C, then the thermal to electric power conversion efficiency will be increased by using a supercritical carbon dioxide (sCO2) Brayton power cycle instead of currently using a steam Rankine cycle for below 600 °C [7]. Simultaneously, it would reduce the capital investment cost by decreasing the quantity of the storage materials and tank size, which helps to reduce the levelised cost of electricity produced (LCOE) by CSP system.

This review article mainly focused on the exploration of different carbonate salt mixtures and their nanofluids available in the literature, which is essential for future high temperature thermal energy storage applications. Molten carbonate salt has received much attention due to its significant thermophysical and chemical properties. The carbonate salts are also suitable for both sensible and latent heat storage applications [8],[9]. In addition, considering the thermophysical properties and corrosion aspects, carbonate salt have an advantage over chloride and fluoride salts, that along with nitrates are also well explored [4]. The carbonate salts are used in various applications such as carbon capture, the electrolyte in fuel cell and

recently in high temperature thermal energy storage application at CSP plants, where the molten salts can be used above 600 °C [10],[11]. Molten carbonate salt has been investigated for future TES applications due to its enormous advantages like high operating temperature, high specific heat capacity, high stability, low vapour pressure, and less corrosion [11].

2. Mechanisms for thermal energy storage

It is worth noting that three main mechanisms of thermal energy storage currently exist [2]:

- Sensible heat storage: the heat stored by adding kinetic energy to the molecules of a material; that is, when its temperature increases but no change of phase occurs. Thus, energy is absorbed while the material temperature raises (charge) and is released when the material cools down (discharge), as depicted in Figure 1. Sensible heat is usually quantified by the specific heat of the material (c_p) and it also depends on the change of temperature (ΔT).

$$Q_{sensible} = m \cdot c_p \cdot \Delta T = \rho \cdot V \cdot c_p \cdot \Delta T \quad (1)$$

- Latent heat storage; conversely it refers to the thermal energy stored by decreasing intermolecular energies through a phase change, with no changes in temperature taking place. Usually, the operation of latent heat materials, also depicted in Figure 1, is based on storing thermal energy during melting (charge) and releasing it when they solidify (discharge). The amount of exchanged energy can be determined by the phase change enthalpy of the material.

$$Q_{latent} = m \cdot \Delta \mathrm{H} = \rho \cdot V \cdot \Delta \mathrm{H} \quad (2)$$

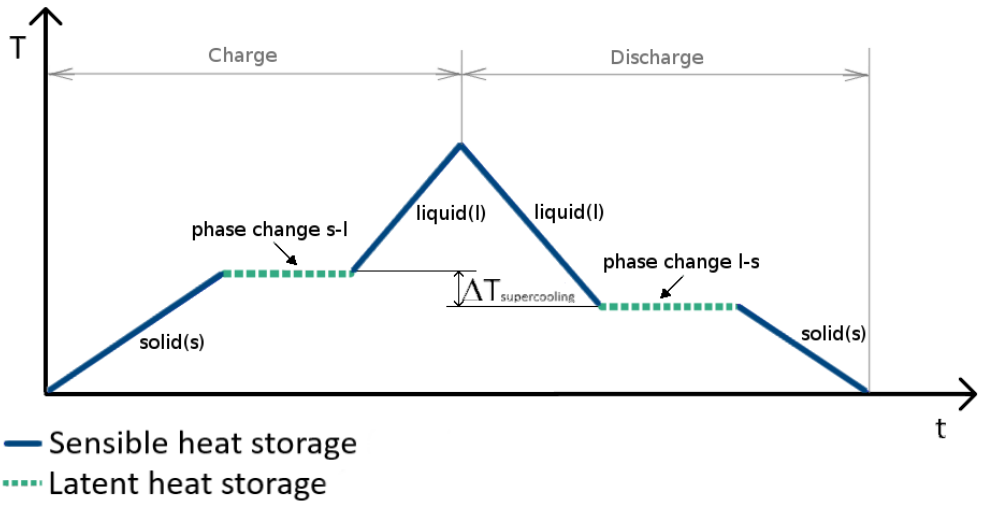

Figure 1. Physical thermal storage mechanisms: sensible and latent heat storage.

- Thermochemical heat storage; thermochemical energy storage is based on the energy stored by breaking chemical bonds during reversible chemical reactions and sorption systems. It has the highest storage capacity, but chemical stability, durability, and the

need for complex storage systems, where products are kept separately, restrict its application in the industry.

Given the particularities of thermochemical heat storage, physical mechanisms for thermal energy storage are the most frequently used in CSP plants, namely sensible and latent heat. Moreover, sensible TES is the traditional thermal energy storage type that is commercially used and found in most current CSP technologies.

3. Materials for thermal energy storage

Besides the operation temperatures of CSP plants, several factors need to be considered to choose the thermal energy storage material [12], [13], such as gravimetric and volumetric storage capacity, thermal conductivity, thermal and chemical stability through cycling, toxicity, flammability, corrosiveness, thermal expansion coefficient or availability, along with cost-related issues. The most important of all these factors are high thermal energy storage capacity to reduce the installation volume while increasing the efficiency, good heat transfer rate that allows fast absorption and release of energy, as well as good stability through thermal cycling, including chemical and thermal stability.

The materials commonly employed for sensible heat storage can be classified according to if they work in the solid or the liquid phase. Those used as TES material when melted include water, thermal oils (mineral or synthetic) or molten salts. In particular, molten salt mixtures can cover a wide range of operating temperatures depending on the composition of the different eutectic and non-eutectic mixtures, with some nitrate-based salts like the well-known solar salt widely used in the solar industry for TES purposes [7] (KNO3-NaNO3 (42-58 mol%)), with a melting temperature of 240 °C; the HitecXL ($Ca(NO_3)_2$-KNO_3-$NaNO_3$ (33.8-51.5-14.7 mol%)), which can work as low as 140 °C [4] or the mixture of KNO_3-$LiNO_3$-$Ca(NO_3)_2$ developed by Zhao and Wu with a melting temperature of 80 °C [14]. For higher temperature, recently, carbonate salts have been identified as a potential candidate for high temperature sensible heat energy storage application in a temperature range from 400 °C to 850 °C, depending on the working atmosphere [15]–[18]. The materials considered for sensible heat storage when solid range from metals to sand or rocks, as well as concrete, ceramics, or even graphite, which can reach operation temperatures up to 2000 °C [19]. They usually come in packed beds in which a flow of HTF is necessary for heat exchange.

With latent heat storage, materials with high phase change enthalpies, known as phase change materials (PCMs), are used. For PCMs with a solid-liquid transition, the optimal material can be chosen by paying attention to its melting temperature and phase change enthalpy according to the working parameters of the desired application. The carbonate based PCM was prepared by using 43 wt.% of Li_2CO_3 and 57wt.% of Na_2CO_3, which shows an enthalpy of 348.5 J/g [20]. Similarly, the ternary carbonates of Li_2CO_3-Na_2CO_3-K_2CO_3 (32.2-33.3-34.5 wt.%) were also studied as PCM materials and it shows a phase change enthalpy of 166 J/g [18]. The materials

more widely used as latent heat storage according to attending their melting temperature and phase change enthalpy are represented in Figure 2.

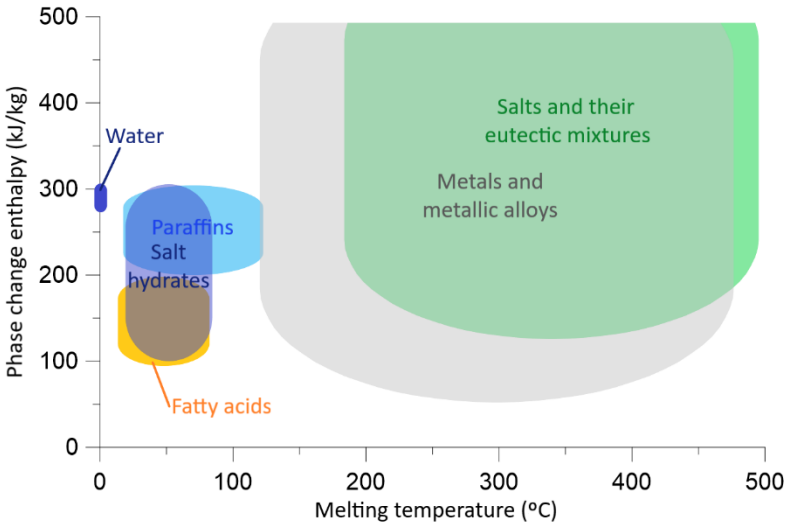

Figure 2. PCM types according to melting temperature and phase change enthalpy [21].

4. Concentrated solar power and molten salts

As previously mentioned, several CSP plant configurations are possible according to the way solar energy is harvested. In line-focusing CSP plants with parabolic trough or linear Fresnel reflectors, harvesting temperatures can range from 0 to 400 °C, whereas point-focusing plants with power tower or parabolic dish collectors can operate at temperatures between 290 °C and 560 °C [22]. These differences lead to different combinations of HTFs and TES materials being employed depending on plant configuration. In line-focusing plants, thermal oils are normally employed as HTF and storage is achieved by including molten salt tanks that act as an indirect storage system (excess heat is first transferred from the HTF to the TES material, and then back to the HTF whenever needed by employing heat exchangers) [2]. Conversely, point-focusing CSP plants may have direct storage systems, that utilise molten salts as both the heat transfer fluid and the thermal energy storage material [3], [23], [24]. Figure 3 depicts schemes of a line-focusing CSP with a parabolic trough configuration and of a point-focusing CSP with a power tower collector.

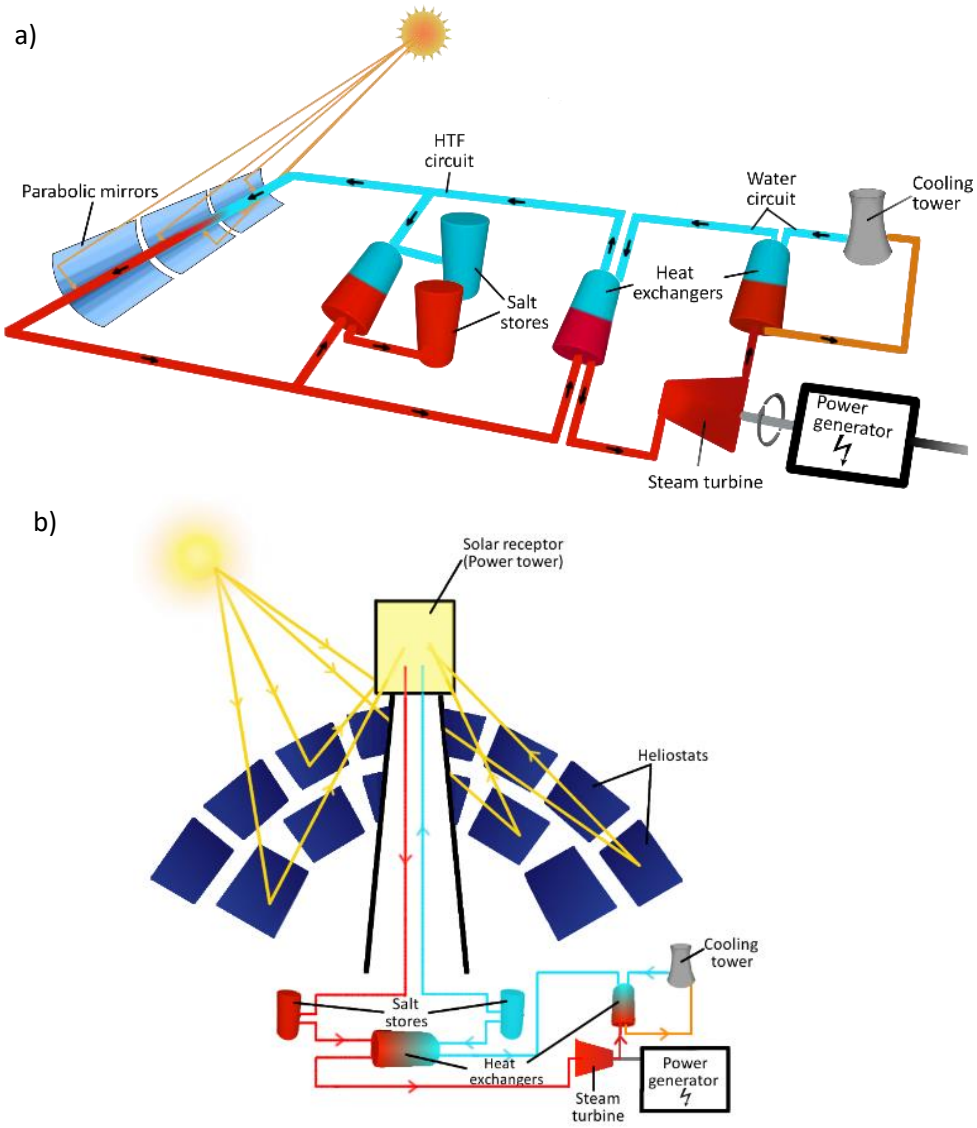

Figure 3. Scheme of CSP plants with (a) parabolic trough and (b) power tower collectors [21].

The total substitution of thermal oil for molten salt can be very advantageous if we take into account that the working temperature of the solar field can increase by enhancing the power block efficiency [25]. In fact, previous literature works suggest that reducing the tank sizes and lacking heat exchangers can make the costs of direct molten salt storage 50% lower than indirect storage [26].

Although some CSP plants use molten salts as HTF, the most widespread configuration still involves having a different fluid such as thermal oil for heat transfer, and using molten salts for thermal energy storage based on their sensible heat when melted. However, molten salts entail some advantages. Mineral oils are highly flammable, which can be a major drawback for their safe use, while synthetic oils are often too expensive [15]. Conversely, molten salts normally present high thermal stability at high temperature and thermal conductivity, and low viscosity, they are non-flammable and non-toxic, and they have a low environmental impact compared to oil.

These advantages, along with the economic benefits of using only one material as HTF and TES, make molten salts ideal materials for CSP technology. Besides, reaching higher temperatures in

CSP plants results in higher efficiencies. However, some other aspects need to be taken into account, such as the salt freezing temperature as a heating aid might be necessary to avoid the solidification of salt through circuits, which can damage the installation, or corrosive interactions with the circuit materials.

Many combinations of anhydrous inorganic salt mixtures have been proposed in the literature for their use in TES and HTF applications. Table 1 summarises the most frequent ones, including their composition, melting temperature (T_m) and maximum working temperature (T_{max}) [22], [27], [28]. Note that the maximum working temperature depends on the experimental conditions of decomposition tests and in some cases a temperature range is provided depending on the test atmosphere (air, argon, nitrogen, etc.). For samples whose T_{max} > 700 °C, the exact experimental value is not provided but at least a maximum working temperature up to 700 °C is ensured.

Table 1. Anhydrous inorganic salt mixtures used for TES and HTF applications [22], [27], [28].

Salt mixture (composition in mol%)	**T_m (°C)**	**T_{max} (°C)**
$LiNO_3$-$Ca(NO_3)_2$-$NaNO_2$-KNO_2 (33-7.7-18.3-41.1) [CaLiNaK]	72	470
KNO_2-KNO_3-$LiNO_3$-$NaNO_2$-$NaNO_3$	95	435
KNO_3-$LiNO_3$-$NaNO_3$ (45.3-36.4-18.3) [LiNaK]	120	435-540
$Ca(NO_3)_2$-KNO_3-$NaNO_3$ (33.8-51.5-14.7) [HitecXL]	140	460-500
KNO_3-$NaNO_2$-$NaNO_3$ (44.2-48.9-6.9) [Hitec]	142	450-540
$LiNO_3$-$NaNO_3$ (54-46)	194	N/A
KNO_3-$NaNO_3$ (50-50)	222	~550
KNO_3-$NaNO_3$ (42-58) [Solar salt]	240	530-560
$NaNO_3$	306	520
KCl-LiCl (41-59)	355	>700
NaF-$NaBF_4$ (7.5-92.5)	385	700
KF-ZrF_4 (57.5-42.5)	390	>700
K_2CO_3-Li_2CO_3-Na_2CO_3 (25.4-43.4-31.2) [LiNaK-CO_3]	397	857
KCl-$MgCl_2$ (66.7-33.3)	426	>700
KF-LiF-NaF (42-46.5-11.5)	454	>700
K_2CO_3-Li_2CO_3 (38-62)	488	600-850
K_2CO_3-Li_2CO_3 (58-42)	498	600-850

According to their melting temperature, molten salts can be classified as:

4.1 Salts with a low melting point (70-200 °C)

When using molten salts as HTF, efforts have been specially made to find mixtures with a low melting point to avoid salts from freezing in the circuit. The salts used for this purpose are mainly nitrates and nitrites, often in ternary, quaternary and even quinary mixtures to reduce melting temperature as low as 72 °C (CaLiNaK sample in Table 1) [22]. Most commonly, the multicomponent mixture has a low melting temperature compared to its individual and binary

salt composition. Because the melting temperature of the molten salt mixture decreases, while the number of ions increases [29].

4.2. Salts with a medium-range melting point (200-350 °C)

As mentioned before, the higher operating temperatures of a CSP plant involve the possibility of greater efficiencies, and allow better thermal energy storage capacity with smaller tank volumes. For those reasons, many works in the literature about thermal energy storage in CSP have focused on the KNO_3-$NaNO_3$ nitrate mixture (42-58 mol%), known as solar salt, whose commercial availability is widespread, is often used as storage media in the present-day, and is occasionally employed as HTF. The composition ratio of solar salt slightly differs from that of the KNO_3-$NaNO_3$ eutectic mixture (50-50 mol%). This difference is due to economic issues, as the cost of $NaNO_3$ is lower than that of KNO_3, and its heat capacity is higher [22]. Therefore, the minor differences in the melting point of both mixtures are considered affordable.

4.3. Salts with a high melting point (>350 °C)

Although the salt mixtures that are more widespread in industry fall within the previous temperature range, this is only due to the current working temperature specifications of solar thermal plants. However, some alternatives proposed in the literature to achieve greater thermal to electric conversion efficiencies require operating at temperatures above 550 °C [30], [31]. When looking for systems that work at high temperatures, the thermal stability of nitrate salts can limit their suitability. For such applications, which can also result in the future of thermal energy storage, salts with a higher melting point are needed, and often in the form of chloride, fluoride or carbonate mixtures. Salts with a high melting temperature also have a high operating temperature, which helps to increase the power cycle efficiency via sCO2 Brayton power cycle. This sCO2 Brayton power cycle has a lower cost with high efficiency compared to the superheated steam-Rankine cycle, while the turbine inlet temperature is above 550 °C [7].

Fluoride mixtures offer relatively high specific heat (similar or even higher than nitrates, carbonates or chlorides depending on the composition [32]–[34]), high thermal conductivity and thermal stability, and their use as nuclear reactor coolants has been researched in the literature [35]. However, their main disadvantages are their cost and their corrosiveness, which are much higher than they are for carbonate and chloride mixtures.

Chloride salts are inexpensive given their abundance, and they present high decomposition temperatures and good thermal stability. Binary mixtures of chlorides usually have lower melting points than carbonate or fluoride salts, but some (e.g. $ZnCl_2$, $AlCl_3$ or $FeCl_2$) also have low boiling points. The molten chloride salt mixture containing Zinc chloride ($ZnCl_2$) has much attention due to its lower melting point, but the high cost of the material makes it less feasible for commercial application [4]. Among the chlorides, the binary molten chloride mixtures of LiCl-RbCl and LiCl-KCl have a lower melting temperature of 313 °C and 355 °C, respectively [36]. Molten chlorides also require making special efforts in the container and installation design because of their extremely corrosive nature in the presence of impurities in atmospheres with oxygen or water [31].

Carbonate mixtures also appear a good alternative as they often present high heat capacity and good thermal stability. In carbonate mixtures that include lithium, their cost is a challenge, due

to the cost of this material being subject to the battery market. However, carbonate mixtures show a good compromise between high specific heat values and low-cost per unit energy. Therefore, when compared with fluorides and chlorides, a high thermal energy storage capacity can be achieved for the same working temperature range, while avoiding the corrosion problems caused by chloride and fluoride mixtures and being cheaper than fluorides [36].

5. Enhancement of molten salt thermal energy storage by using nanofluids

In the molten salts context, other mechanisms to enhance their TES capacity exist apart from the choice of a different salt mixture. Nanofluids are colloidal suspensions of solid particles of nanometric size in a fluid. The Al_2O_3 and SiO_2 nanoparticles were the most commonly used material for the preparation of molten salt-based nanofluids. A low concentration of the nanoparticles such as 0.1, 0.5, 1, 2, and 5 wt.% was added to the base fluids to enhance their thermophysical properties [5]. They were initially proposed for heat transfer applications due to the enhancements in thermal conductivity achieved by adding nanoparticles in the base fluids [37], [38]. However, thermal energy storage capacity enhancements can also be achieved in nanofluids based on ionic liquids, as first reported by Shin and Banerjee in 2011 [39], [40].

This increase in specific heat cannot be predicted according to the specific heats of the base fluid and nanoparticles following the mixture rule. The mechanisms behind it have still not been completely determined and research efforts are being made in this topic [41]. However, three mechanisms are proposed in the literature to explain this increase in specific heat [40]: the first one focuses on the high surface energy added by nanoparticles due to their small size [42], and it has been proposed that specific heat can depend on the nanoparticle diameter [43]. The second mechanism suggests that the interface between nanoparticles and the base fluid presents abnormally good resistance [42], [44]. The third mechanism proposes the presence of a semisolid structured layer that forms around nanoparticles and acts as a specific heat enhancement [45], [46]. In relation to this, one of the most well-accepted hypotheses today is about the ionic interactions between molten salt and nanoparticles in their interphase, which lead to the formation of special nanostructures [47], [48]. These nanostructures that form at the interphase have been observed in nanofluids based on low-temperature organic salts [49].

The first works of Shin and Banerjee used carbonate (K_2CO_3-Li_2CO_3) and chloride ($BaCl_2$-NaCl-$CaCl_2$-LiCl) mixtures as their base fluid for thermal energy storage. However, as other salt mixtures with a lower melting point are more widespread in the industry, such as solar salt, Hitec or HitecXL, many works that have studied nanofluids based on these salts to be used as sensible storage material, HTF or latent heat storage material have been published, and compiled in some literature reviews [50], [51]. Nonetheless, very few works also deal with the inclusion of nanoparticles in molten carbonate mixtures [52], following the example set by Shin and Banerjee and focusing on the future of thermal energy storage at higher operating temperatures. Similarly, the SiO_2 based K_2CO_3-Li_2CO_3 (38:62 molar ratio) nanofluid was prepared by using different sizes of SiO_2 nanoparticles (5, 10, 30, and 60 nm) with 1 wt.% addition to the molten salt [53]. The prepared nanofluids showed an enhanced specific heat value of 1.97 J/g °C for 5 nm, 1.98 J/g °C for 10 nm, 1.95 J/g °C for 30 nm and 2.03 J/g °C for 60 nm [53]. Commonly, the nanoparticles tend to agglomerate in the molten salt due to the high surface energy of the

nanoparticles via Van der Waals attraction force [5]. Therefore, the agglomerated nanoparticle creates the clogging effects in the micro-channels and increasing the pumping power of the CSP system [5]. Apart from the enhancement of thermophysical properties, one should consider the other effects caused by nanoparticles in molten salts as well.

The need to use high-temperature TES materials to increase the efficiency of thermal to electrical conversion and the promising performance of carbonate salts make the study of nanofluids based on molten carbonates very interesting. In addition, the high temperature based molten salt takes a longer time to agglomerate and shows good stability [9]. The following sections of this review attempt to gain more profound insights into the state-of-the-art of characterization techniques and the thermophysical properties of the molten carbonate mixtures of Li_2CO_3 and K_2CO_3. In addition, the main survey of carbonates salt based nanofluids was explained by focusing on the challenges, enhancement mechanism and future developments that these materials offer for high temperature thermal energy storage applications.

6. Thermophysical properties

In order to develop materials that help to increase the thermal energy storage efficiency in CSP plants, several thermophysical properties need to be considered. The melting point of the chosen mixture is a key parameter that needs to match the operating temperatures of the desired application. Thermal conductivity plays a key role in the heat transfer rate that determines how fast the energy absorption and release can take place. Whenever the storage material needs to flow (e.g. through a heat exchanger), viscosity must also be considered as it directly affects pumping costs. Then density, latent heat and specific heat have a direct influence on the material thermal energy storage capacity by defining the installation volume required for a certain energy storage capacity. Therefore, an analysis of the available literature works about these properties for Li_2CO_3-K_2CO_3 mixtures and the nanofluids based on them is presented below.

6.1. Melting point

Among the important thermophysical properties for thermal energy storage materials, melting temperature is critical for both latent and sensible storage media.

In eutectic systems, all the material melts and solidifies immediately at a given temperature, which is lower than the melting point of the constituents. It is worth considering that non-eutectic mixtures have a range of temperatures within which both liquid and solid phases are simultaneously present. In such cases, the maximum liquidus temperature is often taken as the melting temperature for operational purposes because it is the minimum temperature needed to completely melt the mixture.

The amplitude, shape and position of the fusion peaks that can be observed by differential scanning calorimetry (DSC) can provide a lot of information on the different compounds present in a sample and their proportion in the mixture, especially when working with non-eutectic combinations of molten salts.

Figure 4 depicts the phase diagram for the K_2CO_3-Li_2CO_3 binary system. The melting temperatures of lithium and potassium carbonates are 723 °C and 891 °C, respectively. Two different eutectic points are observed for 42% and 62% mole Li_2CO_3. According to Janz and Lorenz [54], the melting point of the K_2CO_3-Li_2CO_3 (58-42 mol%) eutectic is 498 °C, and 488 °C for the K_2CO_3-Li_2CO_3 (38-62 mol%) eutectic. Araki et al. confirmed these values and added the melting point of the equimolar complex $LiK(CO_3)$ – or K_2CO_3-Li_2CO_3 (50-50 mol%) – at 505 °C [55]. These values are well agreement with the phase diagram depicted in Figure 4.

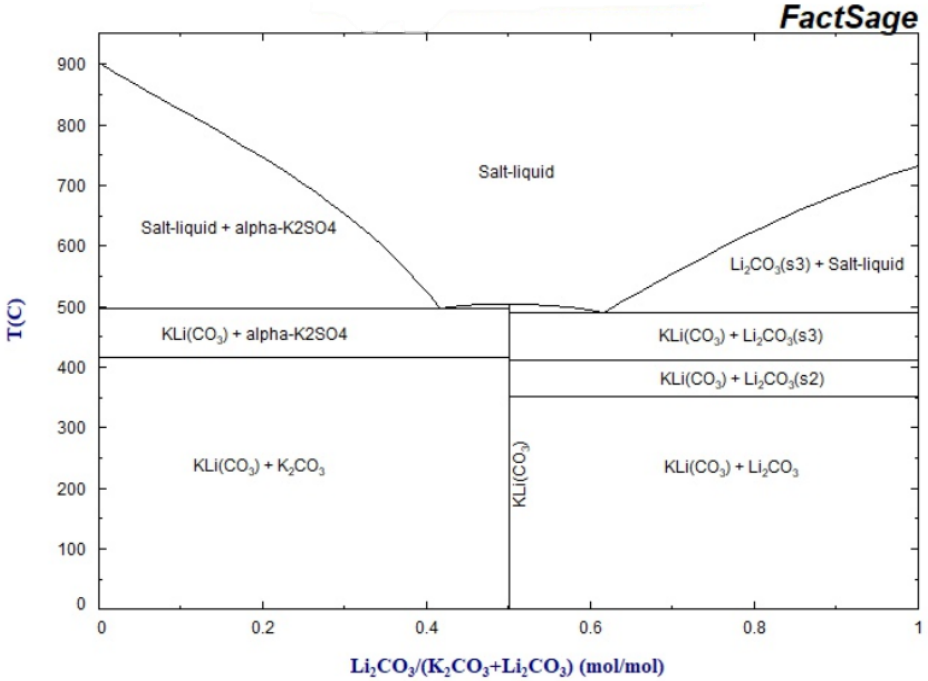

Figure 4. K_2CO_3-Li_2CO_3 binary phase diagram [56].

As for the other non-eutectic combinations of the K_2CO_3-Li_2CO_3 mixture, Jo and Banerjee proved that fusion peaks showed different shapes according to the mole fraction of the lithium carbonate, which was also related to different specific heat values [57].

6.2. Density

Density is present in both thermal conductivity (as seen in Equation 5) and the amount of energy that a certain mass of a material can store (Q), as seen in Equations 1 and 2.

Therefore, density is an important parameter in both heat transfer and thermal energy storage as it affects the size of thermal energy storage systems considerably because a material with a higher density means that a smaller volume is needed to store the same amount of energy.

A complete study on the densities of K_2CO_3-Li_2CO_3 mixtures, using an Archimedian single bob densitometer, was published by Spedding in 1970 [58], and later included in the compilations for molten salt energy storage by Janz et al. [59]. Some measurements taken at room temperature are available in Marianowski and Maru [60], [61], although the technique is not specified. Araki et al. [55] also measured the densities of the K_2CO_3-Li_2CO_3 eutectics and the equimolar $LiK(CO_3)$. Kojima et al. [62] obtained the density of the K_2CO_3-Li_2CO_3 (38-62 mol%)

eutectic by a maximum bubble pressure technique inside a capillary. A summary of these measurements and their results are offered in

Table 2. The values obtained by the different authors are also represented in Figure 5.

A simple mixture rule (Equation 3) tends to be used to calculate the density of multicomponent mixtures, like combinations of several salts, but is also employed for nanofluids, including the base fluid and nanoparticles density values in the literature, as did Shin and Banerjee [63], [64] or Tao et al. [65]. For this reason, to the best of the authors' knowledge, no measurements of the density of K_2CO_3-Li_2CO_3 based nanofluids are available in the literature because the mixture rule is always used for this purpose.

$$\rho_{mixture} = \frac{1}{V_{mixture}} \sum_{i}^{n} V_i \cdot \rho_i \qquad (3)$$

Table 2. Summary of density measurements of K_2CO_3-Li_2CO_3 in the literature.

Reference	Year	Method	Molar ratio K_2CO_3-Li_2CO_3	Nanoparticle type and loading	Temperature range (°C)
Spedding [58]	1970	Archimedian single bob densitometer	Complete range	-	570-981
Marianowski and Maru, Maru et al. [60], [61]	1977	N/A	58-42	-	25
			50-50	-	25
			38-62	-	25
Araki et al. [55]	1988	Buoyancy by Archi-medes' principle	58-42	-	546-792
			50-50	-	527-810
			38-62	-	510-809
Kojima et al. [62]	2013	Maximum bubble pressure	38-62	-	533-869

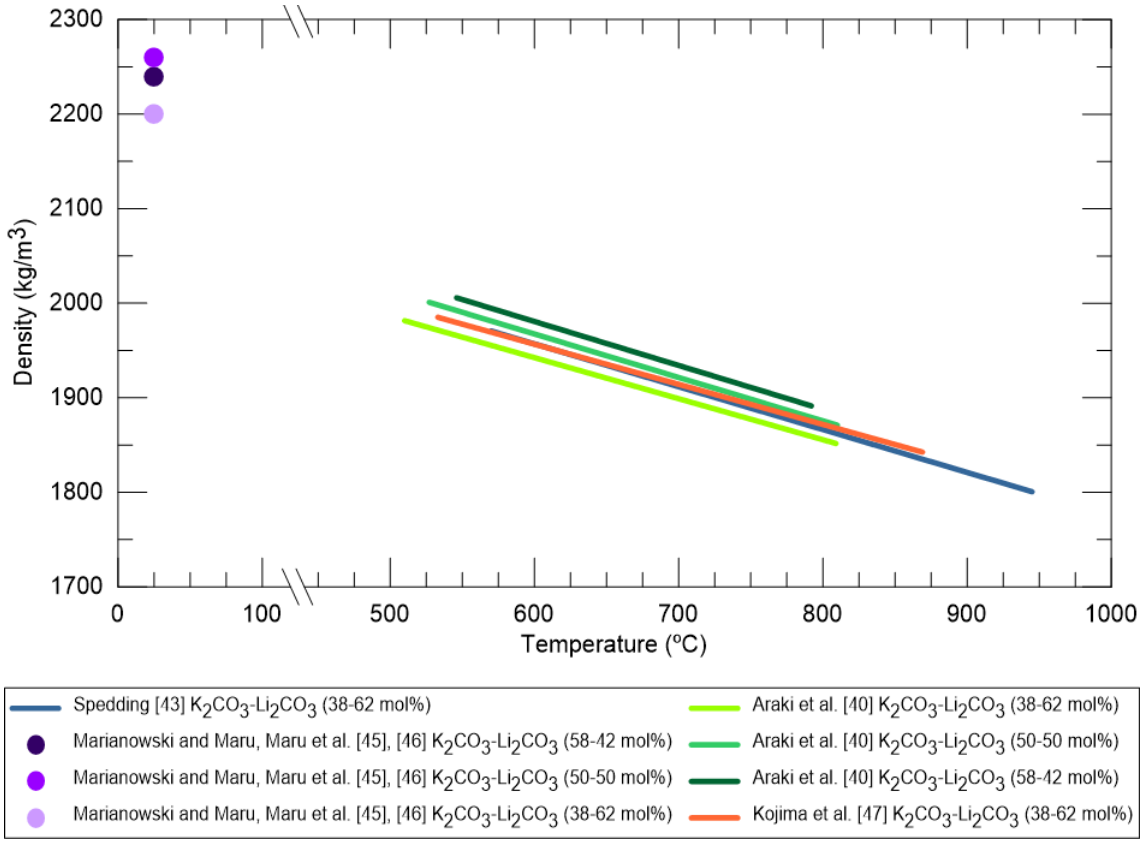

Figure 5. Density measurements of K_2CO_3-Li_2CO_3 available in the literature.

6.3. Viscosity

Viscosity has to be taken into account whenever a fluid needs to be transported through a heat exchanger or any other system. Several methods exist to evaluate the viscosity of media. However, taking measurements of this property at temperatures as high as molten carbonates is not simple. Nothwithstanding, Janz and Saegusa [66] presented the first values of viscosity for pure lithium and potassium carbonates in 1963 by fitting the results they obtained to Arrhenius' equation (Equation 4).

$$\eta = A \cdot e^{E_\eta / RT} \qquad (4)$$

where η is the viscosity of the fluid, A is a constant that depends on the analysed system, E_η is the activation energy, R is the universal constant of gases and T is temperature.

Later, Sato et al. [67] and Di Genova et al. [68] repeated these measurements for pure carbonates (K_2CO_3 and Li_2CO_3), and obtained different results than those reported by Janz and Saegusa [66].

By focusing on the K_2CO_3-Li_2CO_3 mixtures, the compilation of molten salt physical properties from Janz et al. [59] included viscosity measurements of Vorobev et al. [69] for the whole molar concentration range. Maru et al. [61] presented the values for the equimolar K_2CO_3-Li_2CO_3 (50-50 mol%), although the measuring method is not specified. Sato's research group also published viscosity measurements of the K_2CO_3-Li_2CO_3 binary melt and covered the whole molar concentrations range [70], and were followed by Lee et al. [71] and Kim et al. [72] who studied some specific mixtures of the two carbonate salts.

The eutectic mixture K_2CO_3-Li_2CO_3 (38-62 mol%) was also studied by Jo and Banerjee [73], who also measured the viscosity of molten salt-based nanofluids with MWCNT at concentrations from 1 to 5 wt.%. The variations in viscosity that they found very much depended on the nanoparticle concentration, with merely a 6% increase for the nanofluid with MWCNT 1 wt.%, but up to 80% and 1080% for MWCNT 2 wt.% and MWCNT 5 wt.%, respectively. El Far et al. [74] also worked with a K_2CO_3-Li_2CO_3 based nanofluid, including silica nanoparticles and that same nanofluid with the addition of a small amount of NaOH to prevent a dendritic nanostructure from forming around nanoparticles, which is believed to enhance specific heat. The addition of SiO_2 nanoparticles brought about a 34% increase in nanofluid viscosity compared to the base fluid, and this increase was only 8% for the nanofluid with NaOH.

A summary of the viscosity measurements of the K_2CO_3-Li_2CO_3 binary system (including data from pure carbonates) is presented in Table 3, including the method followed and the temperature range studied in each work. The viscosity values obtained by different research groups are depicted in Figure 6.

Table 3. Summary of viscosity measurements of K_2CO_3-Li_2CO_3 and K_2CO_3-Li_2CO_3 based nanofluids in the literature.

Reference	Year	Method	Molar ratio K_2CO_3-Li_2CO_3	Nanoparticle type and loading	Temperature range (°C)
Janz and Saegusa [66]	1963	Oscillating cylinder	100-0 (K_2CO_3)	-	910-985
			0-100 (Li_2CO_3)	-	770-850
Sato et al. [67]	1999	Oscillating cylinder	100-0 (K_2CO_3)	-	906-961
			0-100 (Li_2CO_3)	-	743-925
Di Genova et al. [68]	2016	Rotational rheometer (concentric cylinder)	100-0 (K_2CO_3)	-	910-930
			0-100 (Li_2CO_3)	-	740-900
Vorobev et al. [69]	1966	Oscillating sphere	Complete range	-	700-900
Maru et al. [61]	1978	N/A	50-50	-	530
Sato et al. [70]	1999	Gas injection	22-78	-	637-841
			38-62	-	515-829
			50-50	-	503-828
			70-30	-	676-756
Lee et al. [71]	2013	Falling sphere	60-40	-	507-567
			40-60	-	507-567
Kim et al. [72]	2015	Rotational rheometer (concentric cylinders)	54-46	-	500-850
			50-50	-	550-750
			38-62	-	550-750
			0-100 (Li_2CO_3)	-	730-900
Jo and Banerjee [73]	2014	Rotational rheometer (cone-and-plate)	38-62	-	550
			38-62	MWCNT 1 wt.%	550
			38-62	MWCNT 2 wt.%	550
			38-62	MWCNT 5 wt.%	550
El Far et al. [74]	2020	Rotational rheometer (parallel plates)	38-62	-	540
			38-62	SiO_2 1 wt.%	540
			38-62	SiO_2 1 wt.% + NaOH	540

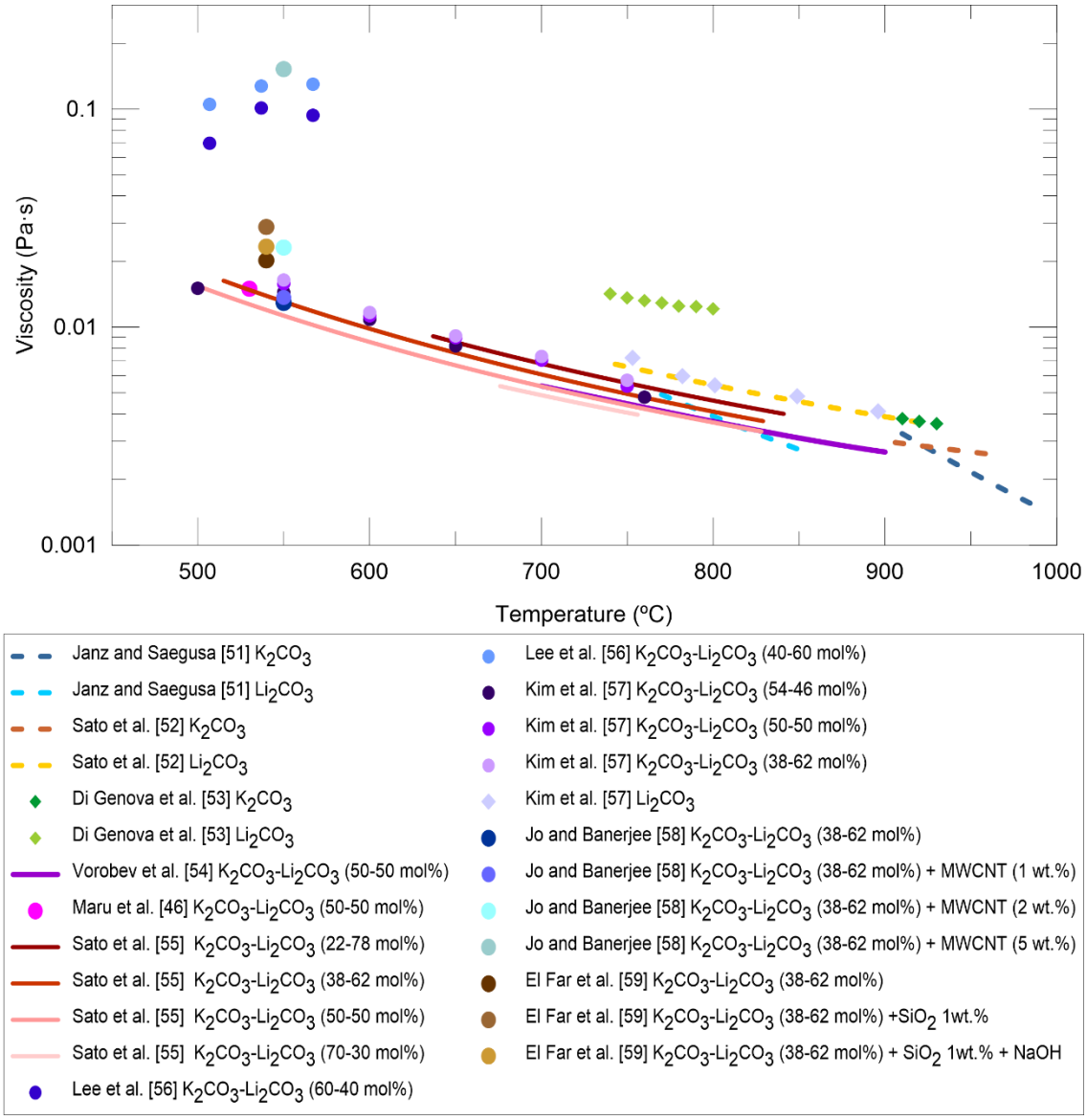

Figure 6. Viscosity measurements of K_2CO_3-Li_2CO_3 and K_2CO_3-Li_2CO_3 based nanofluids available in the literature.

6.4. Thermal conductivity and thermal diffusivity

Thermal conductivity is the key parameter when attempting to improve HTFs, but it also plays a key role for TES materials as the velocity of the charge and discharge processes depends on the heat transfer rate. Thermal conductivity (k) directly depends on thermal diffusivity (α) according to Equation 5

$$k = \alpha \cdot \rho \cdot c_p \qquad (5)$$

where ρ refers to density and c_p to specific heat.

Therefore, high thermal diffusivity results in fast responses to temperature differences in the TES material and, thus, in quick charging and discharging processes.

The review of Kenisarin [75] reports the early measurements of K_2CO_3-Li_2CO_3 eutectics thermal conductivity by Marianowski and Maru [60] and Maru et al.[61]. Later, Araki et al. [55] measured

the thermal diffusivity of both K_2CO_3-Li_2CO_3 eutectics and equimolar LiK(CO_3) and developed correlations for thermal conductivity between 534 °C and 687 °C. Zhang and Fujii [76] measured both thermal diffusivity and thermal conductivity by a transient short-hot-wire method capable of withstanding corrosive media, such as molten carbonates. The data of the pure K_2CO_3 and Li_2CO_3 carbonates can be found in Geyer [77] and Shiina and Inagaki [78], although no details about the measuring method or conditions are provided.

More recently, the research group of Shin and Banerjee also studied the thermal diffusivity of the K_2CO_3-Li_2CO_3 (38-62 mol%) eutectic in the solid state by a laser flash analysis [63], [64]. They also studied a molten salt-based nanofluid containing SiO_2 nanoparticles, and reported enhancements for thermal conductivity of up to 47%. Tao et al. [65] also measured thermal conductivity by a laser flash analysis of nanofluids based on K_2CO_3-Li_2CO_3 (38-62 mol%). They designed these nanofluids as composite phase change materials (CPCM), for which they included SWCNT, MWCNT, Graphene and C_{60} as nanoparticles at different concentrations ranging from 0.1 to 2.5 wt.%. Although they did not report the absolute values of the measured thermal conductivity, they stated enhancements of up to 18.5% in thermal conductivity of nanofluids vs. base salts.

A summary of the thermal conductivity and diffusivity measurements available in the literature for the K_2CO_3-Li_2CO_3 mixtures is presented in Table 4, which includes details of the measurement conditions of each work. A visual representation of the results obtained for thermal conductivity by the different authors is depicted in Figure 7.

Table 4. Summary of thermal conductivity and diffusivity measurements of K_2CO_3-Li_2CO_3 and K_2CO_3-Li_2CO_3 based nanofluids in the literature.

Reference	Year	Measurement	Method	Molar ratio K_2CO_3-Li_2CO_3	Nanoparticle type and loading	Temperature range (°C)
Marianowski and Maru, Maru et al. [60], [61]	1977	Thermal conductivity	TES laboratory unit	58-42	-	N/A
				50-50	-	N/A
				38-62	-	N/A
Araki et al. [55]	1988	Thermal diffusivity	Stepwise heating method	58-42	-	534-687
				50-50	-	532-700
				38-62	-	497-706
Geyer [77]	1991	Thermal conductivity	N/A	100-0 (K_2CO_3)	-	N/A
Zhang and Fujii [76]	2000	Thermal diffusivity and conductivity	Short-hot-wire technique	30-70	-	548-649
Shiina and Inagaki [78]	2005	Thermal conductivity	N/A	0-100 (Li_2CO_3)	-	N/A
Shin and Banerjee [63], [64]	2011	Thermal diffusivity	Laser flash analysis	38-62	-	150-300
				38-62	SiO_2 1 wt.%	150-300
Tao et al. [65]	2015	Thermal diffusivity and conductivity	Laser flash analysis	38-62	-	N/A
				38-62	MWCNT 0.1 wt.%	N/A
				38-62	MWCNT 0.5 wt.%	N/A
				38-62	MWCNT 1 wt.%	N/A
				38-62	MWCNT 1.5 wt.%	N/A
				38-62	MWCNT 2.5 wt.%	N/A

				38-62	SWCNT 0.1 wt.%	N/A
				38-62	SWCNT 0.5 wt.%	N/A
				38-62	SWCNT 1 wt.%	N/A
				38-62	SWCNT 1.5 wt.%	N/A
				38-62	SWCNT 2.5 wt.%	N/A
				38-62	Graphene 0.1 wt.%	N/A
				38-62	Graphene 0.5 wt.%	N/A
				38-62	Graphene 1 wt.%	N/A
				38-62	Graphene 1.5 wt.%	N/A
				38-62	Graphene 2.5 wt.%	N/A
				38-62	C_{60} 0.1 wt.%	N/A
				38-62	C_{60} 0.5 wt.%	N/A
				38-62	C_{60} 1 wt.%	N/A
				38-62	C_{60} 1.5 wt.%	N/A
				38-62	C_{60} 2.5 wt.%	N/A

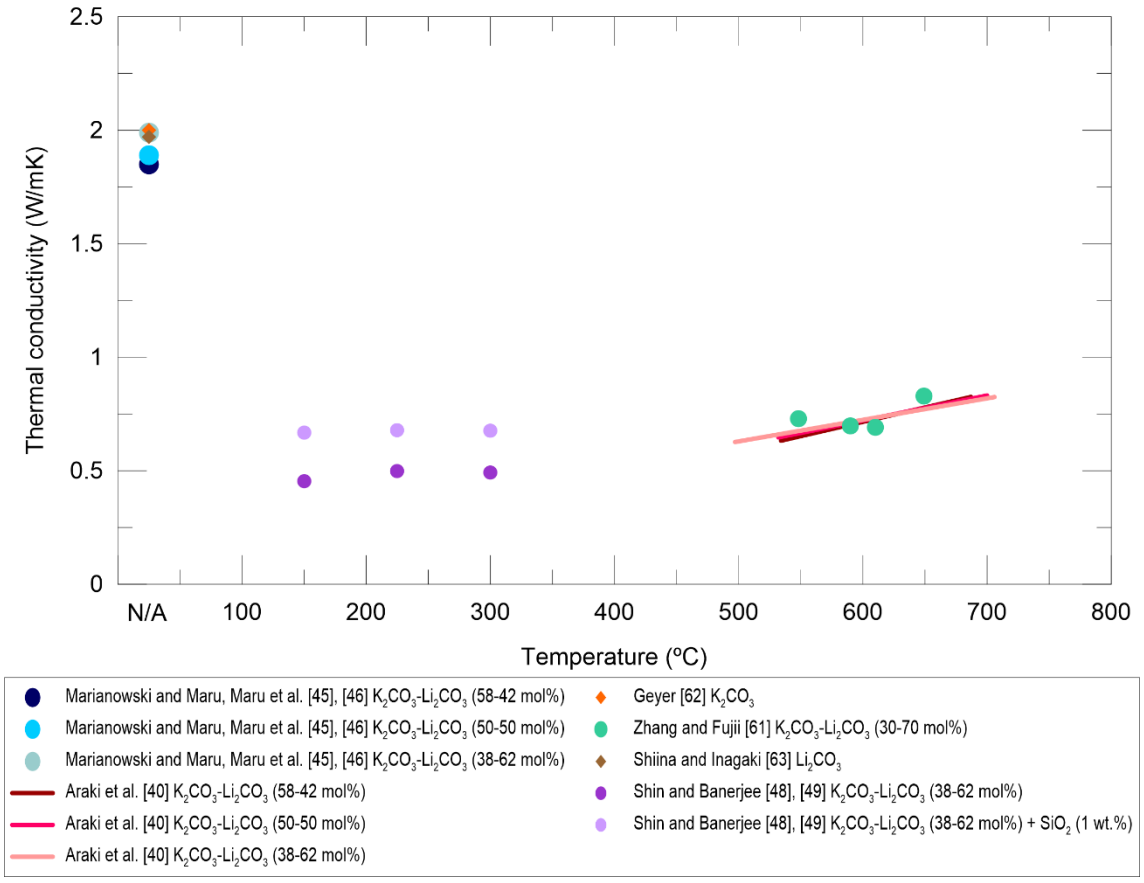

Figure 7. Thermal conductivity measurements of K_2CO_3-Li_2CO_3 and K_2CO_3-Li_2CO_3 based nanofluids available in the literature.

6.5. Latent heat of fusion

One of the most important thermophysical properties in PCMs is the capacity to store thermal energy during their phase change. As the most convenient transformation in PCMs used as TES

material is often solid-liquid, the enthalpy of fusion (also latent heat of fusion) is the property that defines latent storage capacity.

The values of latent heat of fusion of both the K_2CO_3 and Li_2CO_3 pure carbonates were reported by Janz et al. [79] in 1963. The first phase change enthalpy measurements of the K_2CO_3-Li_2CO_3 mixture were published by Janz and Perano [80] for the equimolar mixture (50-50 mol%). The works of Marianowski and Maru [60], and Maru et al. [61] also indicate the values for both eutectic mixtures and the equimolar combination, which agree with the previous literature.

More recently in 2015, Jo and Banerjee [57] studied the latent heat of fusion of the K_2CO_3-Li_2CO_3 binary mixtures at many molar concentrations by differential scanning calorimetry. They also attempted to predict values, based on the latent heat of fusion of the eutectics and the mass fraction of salts in the liquid phase, as the solid remnants in non-eutectic mixtures do not add latent heat of fusion to the mixture. They concluded that these theoretical predictions could be used as a preliminary estimation. However, these predictions were more accurate for compositions that came closer to the eutectic (with errors within the 5-10% range) than for the compositions further away from the eutectics (with errors of up to 23%). In the same year, Liu et al. [81] and Tao et al. [65] also analysed some K_2CO_3-Li_2CO_3 combinations with DSC. The work of Tao et al. included nanofluids based on the eutectic mixture K_2CO_3-Li_2CO_3 (38-62 mol%) and carbon nanoparticles with different structures (SWCNT, MWCNT, Graphene, C_{60}) with mass fractions from 0.1 to 2.5 wt.%, which they designed as composite phase change materials (CPCM). All the nanofluids presented a lower latent heat of fusion than that of the eutectic salt mixture, which the authors attributed to the reduction in the mass fraction of salt (whose place is occupied by nanoparticles), and also to the existence of a nano-layer between nanoparticles and molten salt, which may present a solid or semisolid phase and reduce the fusion enthalpy of nanofluids.

The available literature works on latent heat of fusion, along with the values obtained for the different K_2CO_3-Li_2CO_3 combinations, are presented in Table 5 and Figure 8, respectively.

Table 5. Summary of the latent heat of fusion measurements of K_2CO_3-Li_2CO_3 and K_2CO_3-Li_2CO_3 based nanofluids in the literature.

Reference	Year	Method	Molar ratio K_2CO_3-Li_2CO_3	Nanoparticle type and loading
Janz et al. [79]	1963	High-temperature calorimetric assembly	100-0 (K_2CO_3)	-
			0-100 (Li_2CO_3)	-
Janz and Perano [80]	1964	Drop calorimetry	50-50	-
Marianowski and Maru, Maru et al. [60], [61]	1977	N/A	58-42	-
			50-50	-
			38-62	-
Jo and Banerjee [57]	2015	Differential scanning calorimetry	Wide range (14 combinations)	-
Liu et al. [81]	2015	Differential scanning calorimetry	58-42	-
			55-45	-
Tao et al. [65]	2015	Differential scanning calorimetry	38-62	-
			38-62	MWCNT 0.1 wt.%
			38-62	MWCNT 0.5 wt.%
			38-62	MWCNT 1 wt.%
			38-62	MWCNT 1.5 wt.%

			38-62	MWCNT 2.5 wt.%
			38-62	SWCNT 0.1 wt.%
			38-62	SWCNT 0.5 wt.%
			38-62	SWCNT 1 wt.%
			38-62	SWCNT 1.5 wt.%
			38-62	SWCNT 2.5 wt.%
			38-62	Graphene 0.1 wt.%
			38-62	Graphene 0.5 wt.%
			38-62	Graphene 1 wt.%
			38-62	Graphene 1.5 wt.%
			38-62	Graphene 2.5 wt.%
			38-62	C_{60} 0.1 wt.%
			38-62	C_{60} 0.5 wt.%
			38-62	C_{60} 1 wt.%
			38-62	C_{60} 1.5 wt.%
			38-62	C_{60} 2.5 wt.%

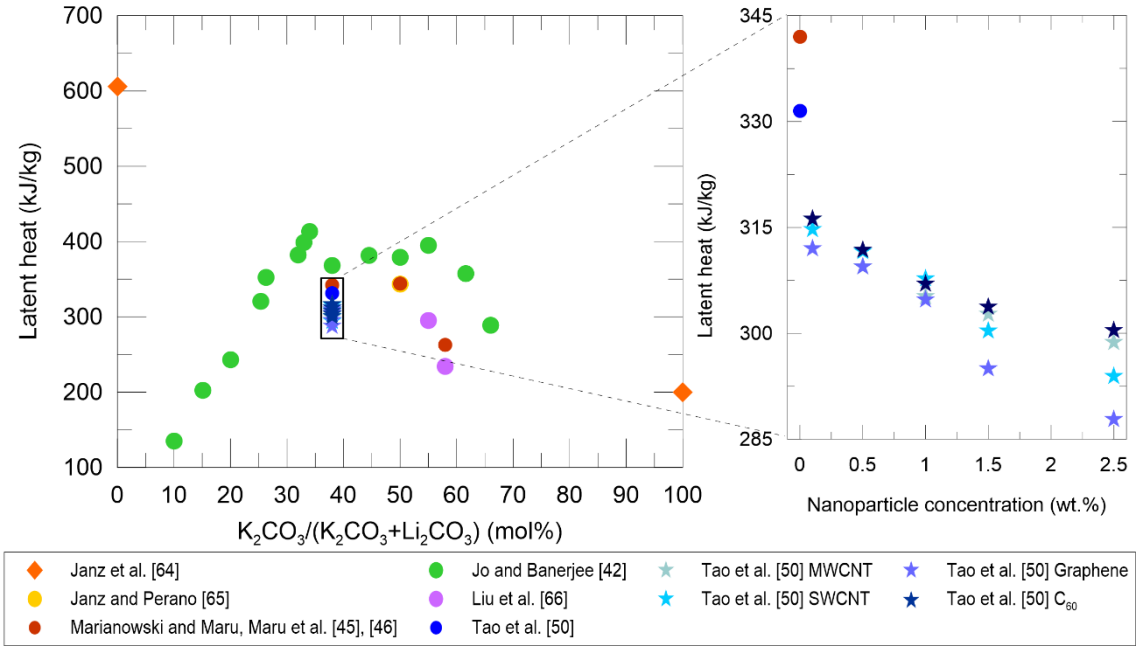

Figure 8. Latent heat of fusion measurements of K_2CO_3-Li_2CO_3 and K_2CO_3-Li_2CO_3 based nanofluids available in the literature.

6.6. Specific heat

Specific heat is the most important property in the materials used for sensible thermal energy storage. It defines how much energy can be stored by a material per unit mass when increasing the temperature by 1 °C. Consequently, many efforts have been made in the literature to study the specific heat of molten salt mixtures, and to enhance it by adding nanoparticles.

As mentioned before, nanofluids were initially meant to increase the thermal conductivity of base fluids. However, in nanofluids based on ionic liquids, such as molten salts, abnormal specific heat enhancement, greater than that which can be predicted by the mixture rule, was achieved

[51]. Therefore, nanofluids have become especially important in the research of molten salts for thermal energy storage purposes.

On the K_2CO_3-Li_2CO_3 molten carbonate mixtures, many authors have studied their specific heat: first came Janz and Perano [80] in 1964, as reflected in Table 6. Most of these measurements focused on the eutectic combinations of K_2CO_3 and Li_2CO_3, or on the equimolar mixture. However, some works centred on studying a wider range of molar ratios, and established that very different values are obtained according to the mixture molar composition [57], [63], [82], [83]. These differences are also observed in Figure 9. First, Shin [63] and then Jo and Banerjee [57] classified these results into three groups according to their composition and specific heat. The first group had a K_2CO_3 molar content below 30% and presented specific heat values above 2.5 kJ/kgK, much higher than eutectics. The second group covered mixtures ranging from the 30% to 38% molar concentrations of K_2CO_3 and the specific heat of the mixtures in this region vastly varied with minor changes in concentration, from 2.5 kJ/kgK to around 1.6 kJ/kgK for a typical value from the eutectic. Finally, the third group comprised salts with a K_2CO_3 molar content above 38% and presented specific heat values closer to 1.5 kJ/kgK. Although this tendency was noted only by a few of the cited authors, Figure 9 shows how all the measurements present in the literature follow this trend. It is also worth noting that, when attempting to measure specific heat in the samples in the second group, very slight changes in composition, which may be due to uneven distribution of K_2CO_3 and Li_2CO_3 in a same sample, can imply very different results and make it especially hard to obtain reliable specific heat measurements in this region.

Table 6. Summary of the specific heat measurements of K_2CO_3-Li_2CO_3 in the literature.

Reference	Year	Method	Molar ratio K_2CO_3-Li_2CO_3	Temperature range (°C)	Specific heat (kJ/kgK)
Janz and Perano [80]	1964	Drop calorimetry	50-50	505-927	1.760
Marianowski and Maru, Maru et al. [60], [61]	1978	N/A	50-50	505	1.760
			58-42	liquid	1.800
			38-62	liquid	1.340
Selman and Maru [84]	1981	N/A	38-62	650	1.600
Araki et al. [55]	1988	Adiabatic scanning calorimeter (ASC)	57-43	488-778	1.490
			50-50	488-778	1.550
			38-62	488-778	1.600
Shin [63]	2011	DSC (ASTM-E1269)	38-62	495-555	1.620-1.650
			54-46	525-555	1.520
			46-54	525-555	1.570
			30-70	525-555	2.900
			22-78	525-555	2.700
Shin and Banerjee [85]	2011	DSC (ASTM-E1269)	38-62	525-555	1.620-1.650
Shin and Banerjee [39]	2011	DSC (ASTM-E1269)	38-62	525-555	1.600
Shin and Banerjee [86]	2013	DSC (ASTM-E1269)	38-62	525-555	1.590
Tiznobaik and Shin [87]	2013	MDSC	38-62	525-555	1.590
Jo and Banerjee [88]	2014	DSC (ASTM-E1269)	38-62	525-550	1.610
			25-75	525-550	2.660

			66-34	525-550	1.320
Jo and Banerjee [89]	2015	DSC (ASTM-E1269)	38-62	525-555	1.610
Jo and Banerjee [57]	2015	DSC (ASTM-E1269)	10-90	525-555	2.580
			15-85	525-555	2.610
			20-80	525-555	2.500
			25-75	525-555	2.660
			26-74	525-555	2.750
			32-68	525-555	2.500
			33-67	525-555	2.090
			34-66	525-555	1.680
			38-62	525-555	1.610
			45-55	525-555	1.510
			50-50	525-555	1.540
			55-45	525-555	1.440
			62-38	525-555	1.290
			66-34	525-555	1.320
Jo and Banerjee [82]	2015	DSC (ASTM-E1269)	21-79	525-555	2.530
			32-68	525-555	2.500
			36-64	525-555	1.680
			58-42	525-555	1.410
			63-37	525-555	1.350
Liu et al. [81]	2015	DSC	72-28	550-700	1.660
			65-35	550-650	1.730
Tao et al. [65]	2015	DSC	38-62	560-580	1.610
Tiznobaik et al. [90]	2015	DSC	38-62	525-555	1.620
Kim and Jo [83]	2018	DSC (ASTM-E1269)	10-90	525-555	2.580
			20-80	525-555	2.500
			25-75	525-555	2.750
			38-62	525-555	1.650
			50-50	525-555	1.540
			60-40	525-555	1.330
Sang et al. [91]	2019	STA	38-62	525-555	1.590
El Far et al. [74]	2020	MDSC	38-62	540	1.510
Rizvi et al. [92]	2020	DSC (ASTM-E1269)	38-62	540	1.570-1.590
Rizvi and Shin [48]	2020	MDSC	38-62	540	1.580

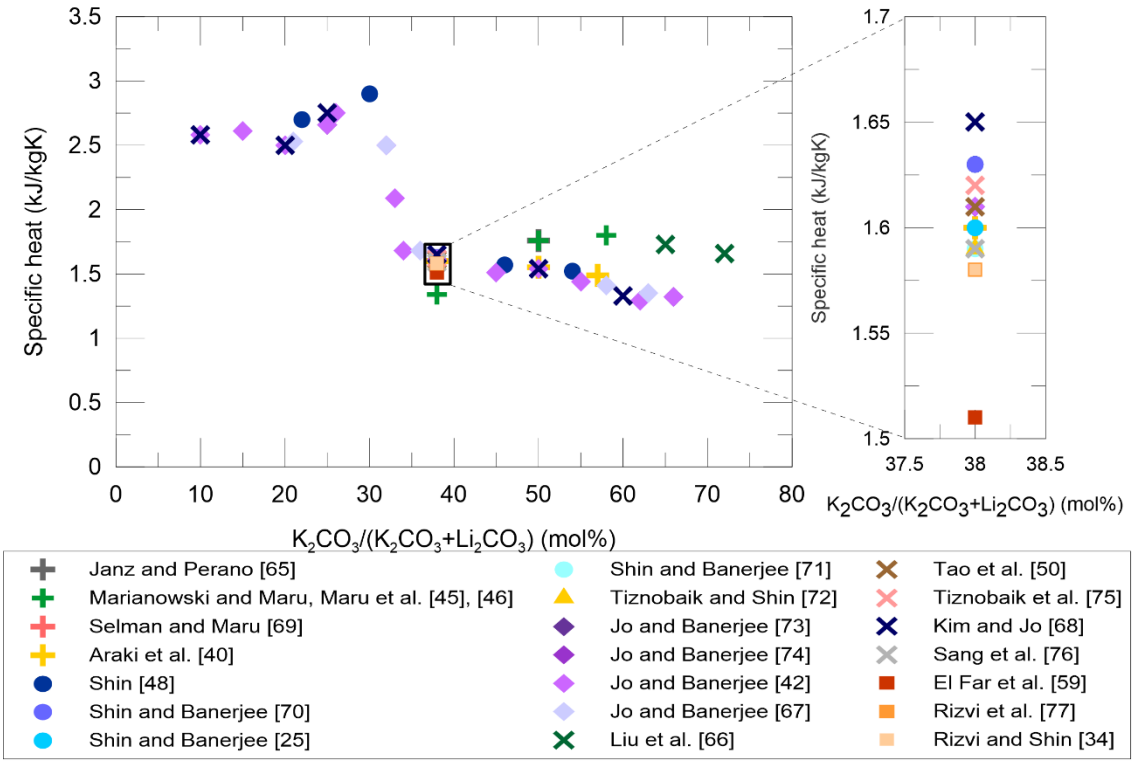

Figure 9. Summary of the specific heat measurements of K_2CO_3-Li_2CO_3 in the literature.

With the K_2CO_3-Li_2CO_3 based nanofluids, several authors have produced them and measured their specific heat in the last decade, as reflected in Table 7, but most come from the research groups at the Texas A&M University and the University of Texas at Arlington. Many types of nanoparticles and nanoparticle loadings have been used to produce these nanofluids, combined with different molar ratios of carbonates for the molten salt mixture. Many of these nanofluids present enhanced specific heat compared to the base fluid (the molten K_2CO_3-Li_2CO_3 mixture in the same proportion). However, not all of them do so and the mechanisms of this possible enhancement are still discussed even today [41]. In 2011, Shin and Banerjee proposed three different mechanisms that could contribute to the abnormal specific heat enhancement recorded in molten salt-based nanofluids (already discussed in Section 5): due to the high specific surface energy of nanoparticles, due to the formation of a semi-solid layer with enhanced thermal properties around nanoparticles, and due to a high interfacial thermal resistance between nanoparticles and molten salts that dominates heat transfer [39], [40].

The specific heat enhancements obtained for K_2CO_3-Li_2CO_3 based nanofluids including different nanoparticles are found in Table 7, and depicted in accordance with the nanoparticle composition in Figure 10 (SiO_2 nanoparticles), Figure 11 (carbon nanoparticles) and Figure 12 (MgO, Al_2O_3 and TiO_2 nanoparticles). These figures display that most nanofluids show specific heat enhancements of up to 30%, regardless of nanoparticle type, and data are scattered even when a same combination of K_2CO_3-Li_2CO_3 molar ratio, nanoparticle type and loading is chosen. It is also worth noting that a few samples show extraordinary enhancements of between 85-125% and always correspond to those nanofluids differentiated as fine powder. A more in-depth analysis of this phenomenon is presented in Section 6.6.2 and Figure 13.

It is worth noteworthy that many K_2CO_3-Li_2CO_3 based nanofluids found in the literature contain a concentration of 1 wt.% nanoparticles. This amount is traditionally used in molten salt-based nanofluids as it has been proven to result in maximum specific heat enhancement [93]. This

phenomenon is believed to be due to the compromise between the nanoparticle effect on the formation of structures that contribute to increased specific heat and the agglomeration of these nanoparticles, which results in a smaller available interfacial surface area which hinders that enhancement [94], [95].

Moreover, the effect of adding NaOH to nanofluids to prevent these nanostructures from forming has also been studied in the works by Tiznobaik and Shin [96], El Far et al. [74], Rizvi et al. [92] and Rizvi and Shin [48]. In the works of Shin [63] and Shin and Banerjee [86], two different regions were observed in nanofluids, namely coarse and fine powder, and a later analysis of the composition of one of the samples determined that the molar ratio of K_2CO_3-Li_2CO_3 had slightly changed. However, no data on the final composition of the other samples were provided. So they are included in the table with the initial base salt composition used (38-62 mol%) in Table 7. Finally, the effect of different heating/cooling rates on the synthesis of nanofluids was also studied by Rizvi et al. [92]. All these phenomena and their effect on the specific heat of nanofluids are explained in more detail in the sections below.

Table 7. Summary of the specific heat measurements of K_2CO_3-Li_2CO_3 based nanofluids in the literature.

Reference	Year	Method	Molar ratio K_2CO_3-Li_2CO_3	Nanoparticle type and loading	Temperature range (°C)	Specific heat (kJ/kgK)	Specific heat enhancement
Shin [63]	2011	DSC (ASTM-E1269)	38-62	SiO_2 1 wt.%	495-555	1.930-2.030	19-23%
			54-46	SiO_2 1 wt.%	525-555	1.440	-5%
			46-54	SiO_2 1 wt.%	525-555	1.530	-3%
			30-70	SiO_2 1 wt.%	525-555	3.260	12%
			22-78	SiO_2 1 wt.%	525-555	2.720	1%
			36-64 (coarse)	SiO_2 1 wt.%	525-555	1.490-1.690	-8-2%
			27-73 (fine)	SiO_2 1 wt.%	525-555	3.280-3.560	102-116%
			38-62* (coarse)	MgO 1 wt.%	525-555	1.810-2.130	12-29%
			38-62* (fine)	MgO 1 wt.%	525-555	3.030-3.350	87-103%
			38-62* (coarse)	Al_2O_3 1 wt.%	525-555	1.840-1.930	14-17%
			38-62* (fine)	Al_2O_3 1 wt.%	525-555	3.250-3.420	101-107%
Shin and Banerjee [85]	2011	DSC (ASTM-E1269)	38-62	SiO_2 1 wt.%	525-555	1.930-2.030	19-23%
Shin and Banerjee [39]	2011	DSC (ASTM-E1269)	38-62	TiO_2 1 wt.%	525-555	2.000	25%
Shin and Banerjee [86]	2013	DSC (ASTM-E1269)	38-62* (coarse)	SiO_2 1 wt.%	525-555	1.570-1.690	-1-6%
			38-62* (fine)	SiO_2 1 wt.%	525-555	3.460-3.560	118-124%
Tiznobaik and Shin [87]	2013	MDSC	38-62	SiO_2 1 wt.%	525-555	1.950-2.010	23-26%
Tiznobaik and Shin [96]	2013	MDSC	38-62	SiO_2 1 wt.% + NaOH	525-550	1.640	3%
Jo and Banerjee [88]	2014	DSC (ASTM-E1269)	25-75	Graphite 0.1 wt.% (method 1)	525-550	3.120	17%

			66-34	Graphite 0.1 wt.% (method 1)	525-550	2.070	57%
			25-75	Graphite 0.1 wt.% (method 2)	525-550	2.900	9%
			66-34	Graphite 0.1 wt.% (method 2)	525-550	1.690	28%
Shin and Banerjee [97]	2014	DSC	38-62	Al_2O_3 1 wt.%	525-555	2.160-2.200	31-33%
Jo and Banerjee [89]	2015	DSC (ASTM-E1269)	38-62	CNT 0.1 wt.%	525-555	1.660	3%
			38-62	CNT 0.5 wt.%	525-555	1.730	7%
			38-62	CNT 1 wt.%	525-555	1.790	11%
			38-62	CNT 5 wt.%	525-555	1.850	15%
Jo and Banerjee [82]	2015	DSC (ASTM-E1269)	21-79	MWCNT 1 wt.%	525-555	3.270	29%
			32-68	MWCNT 1 wt.%	525-555	3.020	21%
			36-64	MWCNT 1 wt.%	525-555	1.780	6%
			58-42	MWCNT 1 wt.%	525-555	1.700	21%
			63-37	MWCNT 1 wt.%	525-555	1.710	27%
Tao et al. [65]	2015	DSC	38-62	MWCNT 0.1 wt.%	560-580	1.680	4%
			38-62	MWCNT 0.5 wt.%	560-580	1.750	9%
			38-62	MWCNT 1 wt.%	560-580	1.790	11%
			38-62	MWCNT 1.5 wt.%	560-580	1.850	15%
			38-62	MWCNT 2.5 wt.%	560-580	1.830	14%
			38-62	SWCNT 0.1 wt.%	560-580	1.690	5%
			38-62	SWCNT 0.5 wt.%	560-580	1.750	9%
			38-62	SWCNT 1 wt.%	560-580	1.820	13%
			38-62	SWCNT 1.5 wt.%	560-580	1.850	15%
			38-62	SWCNT 2.5 wt.%	560-580	1.810	12%
			38-62	Graphene 0.1 wt.%	560-580	1.720	7%
			38-62	Graphene 0.5 wt.%	560-580	1.780	11%

			38-62	Graphene 1 wt.%	560-580	1.850	15%
			38-62	Graphene 1.5 wt.%	560-580	1.910	19%
			38-62	Graphene 2.5 wt.%	560-580	1.790	11%
			38-62	C_{60} 0.1 wt.%	560-580	1.650	2%
			38-62	C_{60} 0.5 wt.%	560-580	1.720	7%
			38-62	C_{60} 1 wt.%	560-580	1.760	9%
			38-62	C_{60} 1.5 wt.%	560-580	1.780	11%
			38-62	C_{60} 2.5 wt.%	560-580	1.810	12%
Tiznobaik et al. [90]	2015	DSC	38-62	MgO 1 wt.%	525-555	1.970	22%
Kim and Jo [83]	2018	DSC (ASTM-E1269)	10-90	Graphite 0.1 wt.%	525-555	3.100	20%
			20-80	Graphite 0.1 wt.%	525-555	2.860	14%
			38-62	Graphite 0.1 wt.%	525-555	1.760	7%
			50-50	Graphite 0.1 wt.%	525-555	1.730	12%
			60-40	Graphite 0.1 wt.%	525-555	1.610	21%
			10-90	Graphite 1 wt.%	525-555	3.240	26%
			20-80	Graphite 1 wt.%	525-555	3.120	25%
			38-62	Graphite 1 wt.%	525-555	1.780	8%
			50-50	Graphite 1 wt.%	525-555	1.780	16%
			60-40	Graphite 1 wt.%	525-555	1.720	29%
			25-75	Graphite 0.0025 wt.%	525-555	2.820	3%
			25-75	Graphite 0.05 wt.%	525-555	3.030	10%
			25-75	Graphite 0. 1 wt.%	525-555	3.110	13%
			25-75	Graphite 1 wt.%	525-555	3.130	14%
El Far et al. [74]	2020	MDSC	38-62	SiO_2 1 wt.%	540	1.790	19%
			38-62	SiO_2 1 wt.% + NaOH	540	1.640	9%
Rizvi et al. [92]	2020	DSC (ASTM-E1269)	38-62	Al_2O_3 1 wt.%	540 (2°C/min)	1950	23%
			38-62	Al_2O_3 1 wt.%	540 (4°C/min)	1.800	14%
			38-62	Al_2O_3 1 wt.%	540 (6°C/min)	1.720	9%

			38-62	Al_2O_3 1 wt.%	540 (8°C/min)	1.770	12%
			38-62	Al_2O_3 1 wt.%	540 (10°C/min)	1.620	3%
			38-62	Al_2O_3 1 wt.% + NaOH	540 (2°C/min)	1.610	2%
Rizvi and Shin [48]	2020	MDSC	38-62	SiO_2 1 wt.%	540	1.940	23%
			38-62	SiO_2 1 wt.% + NaOH	540	1.610	2%

* The initial composition of the base salt used is indicated despite the differentiation between coarse and fine powders in [63] and [86].

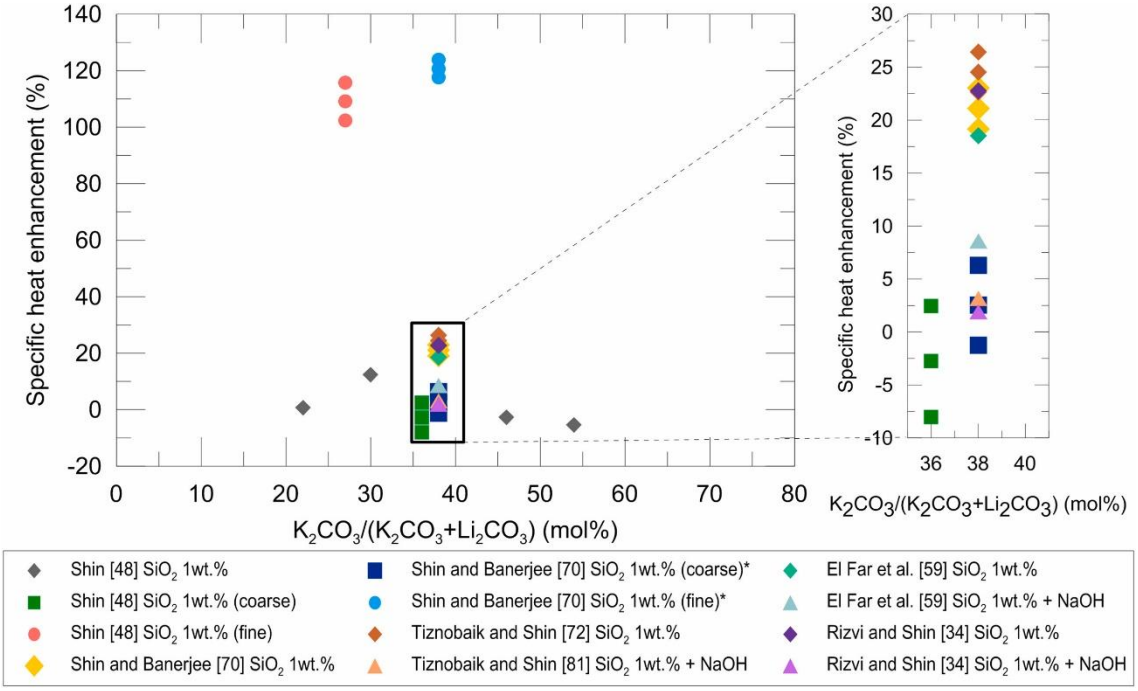

Figure 10. Specific heat enhancement of the K_2CO_3-Li_2CO_3 based nanofluids with SiO_2 nanoparticles.

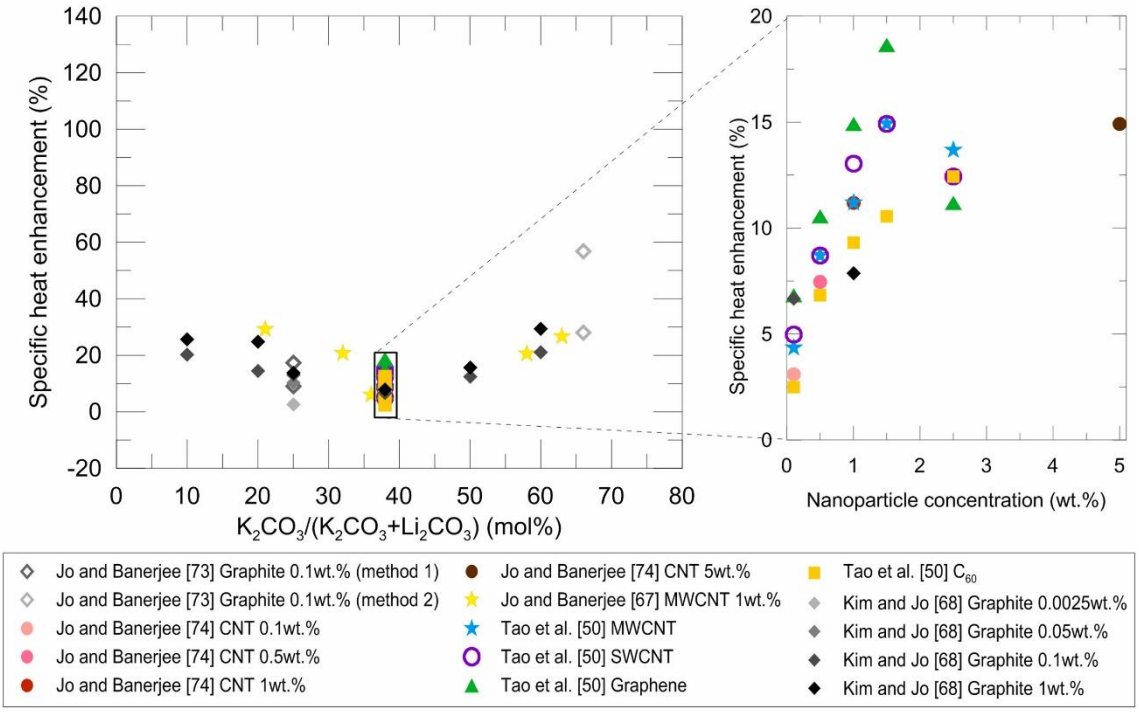

Figure 11. Specific heat enhancement of the K_2CO_3-Li_2CO_3 based nanofluids with carbon nanoparticles.

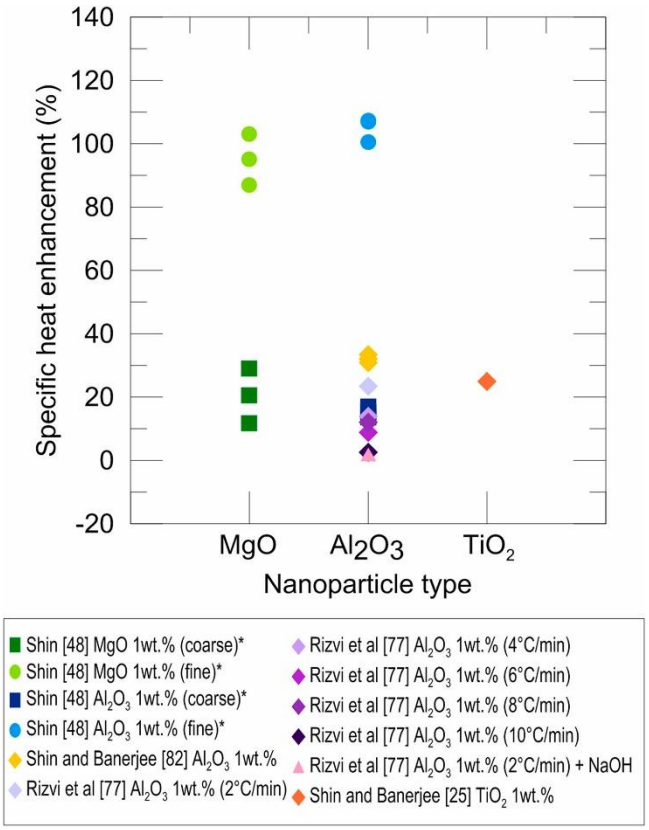

Figure 12. Specific heat enhancement of the K_2CO_3-Li_2CO_3 (38-62) based nanofluids with MgO, Al_2O_3 and TiO_2 nanoparticles.

6.6.1. Possible mechanisms for specific heat enhancement in nanofluids: formation of nanostructures

As for the mechanisms that explain specific heat enhancement, the formation of characteristic structures in the molten carbonate mixtures with nanoparticles was first observed by Shin and Banerjee [85], who detected a percolation network in a SiO_2 nanofluid. This observation was extended by Shin [63] with the formation of needle-like and weave-patterned structures as part of the SiO_2, MgO and Al_2O_3 nanofluids, which displayed greater specific heat enhancement than other nanofluids without them. Similar analyses were published following works by the same authors [86], [87], [92], [97], and summarised up by Tiznobaik et al. in 2015 [90] by directly relating the presence of these needle-like structures to specific heat enhancements and attributing it to them being very large surface areas with a slightly different composition ratio to the salt eutectic, which matched the different densities observed by backscattered electron imaging in SEM. It is worth noting that these kinds of needle-like structures have only been observed to date in carbonate mixtures, and not in other molten salts. The relation between the nanostructure and specific heat enhancement has also been analysed by inhibiting its formation with NaOH [96]. The authors proposed that the cause of the nanostructure formation lie in the difference of electrostatic attractions between nanoparticles and molten salts, and that the addition of the hydroxide groups in NaOH would limit the interactions between them and inhibit the formation of nanostructures and, thus, specific heat enhancement. More recently, this phenomenon has been studied in more depth by Rizvi and Shin [48]. They explain the formation of dendritic structures as being due to microsegregation between the binary carbonate mixture caused by the differences between their electrostatic interaction with nanoparticles. This can be the cause for a disruption in the eutectic composition around particles, and molten salt would start to crystallise around them, and grow into dendrites due to thermophoretic effects.

6.6.2. Variation in the specific heat in nanofluids according to the production method

The influence of the production method on carbonate-based nanofluids has already been studied in the literature for ternary mixtures [98], [99]. With K_2CO_3-Li_2CO_3 mixtures, the work of Shin [63] introduced another particularity of carbonate-based nanofluids. When nanofluids were prepared by the two-step method (dissolving salts in water, then ultrasonically dispersing nanoparticles and drying the sample), and samples were dried on Petri dishes, two different areas of the dried salt-based nanofluid were present: one in the centre that looked coarse and one in the surroundings that looked finer. Individually studying the nanofluids of these two regions showed that the composition ratio of carbonates had differently shifted in each one, and they presented different structures when observed by SEM (with needle-like structures appearing only in “fine” powder). Moreover, the specific heat values were different and much greater enhancements (~100%) were achieved for fine powders. The same phenomenon was later studied in the works by Shin and Banerjee [86], Jo and Banerjee [82], [88] and Kim and Jo [83]. It is worth remarking that nanofluids can appear to not present any specific heat enhancements compared to the base fluid, but improvements are actually recorded compared to the correct K_2CO_3-Li_2CO_3 ratio [88]. Figure 13, is a summary of the measurements found in the literature that differentiate between these coarse and fine nanofluids. It is noted that the nanofluids that look fine always present a higher specific heat value, but the compositional analysis of samples after drying them was only performed in one of them (Shin [63] SiO_2 1 wt.%). Thus possible swifts in the composition ratio of molten salts could have taken place in the other samples. This means that specific heat enhancement would not be as extreme if that change had sufficed to take a molar ratio in the region with higher specific heat (with a K_2CO_3 molar

content below 30%). The work by Jo and Banerjee [88] also detected that when drying nanofluid samples in a small vial instead of a Petri dish, no variations in salt composition were recorded, but specific heat enhancement was lower for the nanofluids dried in a small vial (up to 28%) than for those dried in a Petri dish (up to 57%). This fact was attributed to the shorter dehydration process duration.

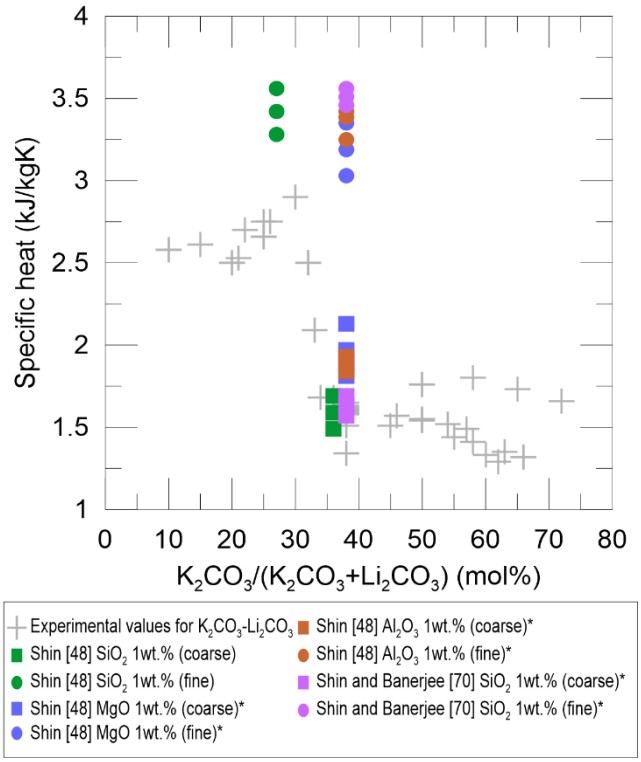

Figure 13. Comparison of the results obtained by Shin and Shin and Banerjee in coarse/fine nanofluids with the experimental values obtained for K_2CO_3-Li_2CO_3 mixtures.

A different aspect whose influence on specific heat enhancement has been studied is the heating/cooling rate applied to samples before measurements. Rizvi et al. [92] compared the effect of applying thermal cycles on a DSC ranging from 2 °C/min to 10 °C/min to both base fluid and nanofluid samples. Their results showed that the heating/cooling rate had no effect on the molten carbonate mixture without nanoparticles, but considerably affected the specific heat of nanofluids, with greater enhancements observed for slower heating/cooling rates. However, this variation was not present when a small quantity of NaOH (which inhibited the formation of a nanostructure, as previously mentioned) was added to nanofluids, which generally displayed no nanofluid specific heat enhancement vs. the base fluid. By relating these findings to the formation of a dendritic nanostructure, the authors also proposed that its extent was related to the heating/cooling rates applied through the synthesis, and that lower velocities favoured the formation of dendrites in nanofluids.

7. Conclusions

The present article offers a state-of-the-art review of the thermophysical properties of potassium and lithium carbonates mixtures for their use as thermal energy storage materials at high temperature. Among the different possibilities of molten salts used in TES, carbonates offer a higher working temperature range than the normally used nitrates, which allows for higher

thermal energy to electricity conversion when designing storage units. They are also more cost-effective than fluorides and present fewer corrosion issues than chlorides, and are one of the best options to continue researching future energy storage alternatives to further increase the efficiency of solar thermal plants and advanced energy processes.

The article offers an analysis of the available literature on the thermophysical properties that play a key role in volumetric thermal energy storage and heat transfer rates: melting point, density, viscosity, thermal conductivity, latent heat of fusion, and specific heat.

The use of nanofluids based on molten carbonates is also reviewed, especially for their specific heat, as the analysis of the other properties comes over less in the literature. Many works have, however, studied abnormal increases in molten carbonate salts when introducing nanoparticles.

The density and thermal conductivity measurements of K_2CO_3-Li_2CO_3 mixtures are scarce, and are sometimes, dispersed, which often responds to very different experimental conditions. The same can be stated of the available viscosity measurement results, which are more numerous. Thus the most suitable values can be chosen from the reviewed data according to the characteristics of the applications to be researched in the future.

For the latent heat of fusion and specific heat, a strong dependence on the molar ratio of the molten salt is observed in the different available works. The specific heat case is especially remarkable as variations in the production method, such as the drying process or the cycling rates applied to the carbonate mixtures or carbonate-based nanofluids, can have a considerable effect on this property. The addition of nanoparticles, mainly oxides (SiO_2, Al_2O_3, MgO or TiO_2) and carbon-based (MWCNT, SWCNT, graphite, graphene and C_{60}) ones, has also been reported to be responsible for specific heat enhancements that cannot be predicted by the traditional mixture rule (with scattered data mainly between 0-30% and some works reporting enhancements of up to 100-120%), and some works proposed these increases to be due to the nanoparticles promoting the formation of special nanostructures in molten salts.

Although more research is needed into the mechanisms that lie behind thermophysical properties enhancement in nanofluids and into the characterisation of these properties at high temperature, the advanced capacities that these materials offer for high-temperature thermal energy storage can play a key role in the future sustainable energy development.

Acknowledgements

The authors wish to thank the financial support from the Ministerio de Economía y Competitividad (MINECO) of Spain (Project ENE2016-77694-R). Nithiyanantham Udayashankar acknowledges the Ministerio de Ciencia e Innovación of Spain for a postdoctoral grant “Juan de la Cierva-formación 2020” (Ref. FJC2020-043416-I). This work was partially funded by the Ministerio de Ciencia, Innovación y Universidades - Agencia Estatal de Investigací on (AEI) (RED2018-102431-T).

REFERENCES

[1] IPCC, “Climate Change 2014 Synthesis Report Summary Chapter for Policymakers,” 2014. doi: 10.1017/CBO9781107415324.

[2] A. Gil *et al.*, “State of the art on high temperature thermal energy storage for power generation. Part 1-Concepts, materials and modellization,” *Renew. Sustain. Energy Rev.*, vol. 14, no. 1, pp. 31–55, 2010, doi: 10.1016/j.rser.2009.07.035.

[3] R. I. Dunn, P. J. Hearps, and M. N. Wright, “Molten-salt power towers: Newly commercial concentrating solar storage,” *Proc. IEEE*, vol. 100, no. 2, pp. 504–515, 2012, doi: 10.1109/JPROC.2011.2163739.

[4] A. Caraballo, S. Galán-Casado, Á. Caballero, and S. Serena, “Molten salts for sensible thermal energy storage: A review and an energy performance analysis,” *Energies*, vol. 14, no. 4, pp. 1–15, 2021, doi: 10.3390/en14041197.

[5] W. Wang, Z. Wu, B. Li, and B. Sunde, “A review on molten-salt-based and ionic-liquid-based nanofluids for medium-to-high temperature heat transfer,” vol. 0123456789, pp. 1037–1051, 2019, doi: 10.1007/s10973-018-7765-y.

[6] A. Limitations and P. Solutions, “Thermal Energy Storage in Solar Power Plants : A Review of the Materials , Associated Limitations , and,” pp. 1–19, 2019.

[7] C. S. Turchi, J. Vidal, and M. Bauer, “Molten Salt Power Towers Operating at 600°C to 650°C : Salt Selection and Cost Benefits Keywords,” *Sol. Energy*, vol. 164, pp. 38–46, 2018.

[8] J. Lee and B. Jo, “Synthesis and Thermal Performance of Microencapsulated Binary Carbonate Molten Salts for Solar Thermal Energy Storage,” *Energy & Fuels*, vol. 35, no. 17, pp. 14130–14139, 2021, doi: 10.1021/acs.energyfuels.1c01763.

[9] X. Chen, Y. ting Wu, L. di Zhang, X. Wang, and C. fang Ma, “Experimental study on thermophysical properties of molten salt nanofluids prepared by high-temperature melting,” *Sol. Energy Mater. Sol. Cells*, vol. 191, no. November 2018, pp. 209–217, 2019, doi: 10.1016/j.solmat.2018.11.003.

[10] D. Corradini, F. X. Coudert, and R. Vuilleumier, “Insight into the Li2CO3-K2CO3 eutectic mixture from classical molecular dynamics: Thermodynamics, structure, and dynamics,” *J. Chem. Phys.*, vol. 144, no. 10, 2016, doi: 10.1063/1.4943392.

[11] G. Pan *et al.*, “Thermal performance of a binary carbonate molten eutectic salt for high-temperature energy storage applications,” *Appl. Energy*, vol. 262, no. October 2019, p. 114418, 2020, doi: 10.1016/j.apenergy.2019.114418.

[12] T. Bauer, W.-D. Steinmann, D. Laing, and R. Tamme, “Thermal Energy Storage Materials and Systems,” *Annu. Rev. Heat Transf.*, vol. 15, no. 15, pp. 131–177, 2012, doi: 10.1615/annualrevheattransfer.2012004651.

[13] Y. Tian and C. Y. Zhao, “A review of solar collectors and thermal energy storage in solar thermal applications,” *Appl. Energy*, vol. 104, pp. 538–553, 2013, doi: 10.1016/j.apenergy.2012.11.051.

[14] C. Y. Zhao and Z. G. Wu, “Thermal property characterization of a low melting-temperature ternary nitrate salt mixture for thermal energy storage systems,” *Sol. Energy Mater. Sol. Cells*, vol. 95, no. 12, pp. 3341–3346, 2011, doi: 10.1016/j.solmat.2011.07.029.

[15] L. A. Weinstein, J. Loomis, B. Bhatia, D. M. Bierman, E. N. Wang, and G. Chen,

"Concentrating Solar Power," *Chem. Rev.*, vol. 115, no. 23, pp. 12797–12838, 2015, doi: 10.1021/acs.chemrev.5b00397.

[16] Y. ting Wu, N. Ren, T. Wang, and C. fang Ma, "Experimental study on optimized composition of mixed carbonate salt for sensible heat storage in solar thermal power plant," *Sol. Energy*, vol. 85, no. 9, pp. 1957–1966, 2011, doi: 10.1016/j.solener.2011.05.004.

[17] R. I. Olivares, C. Chen, and S. Wright, "The thermal stability of molten lithium-sodium-potassium carbonate and the influence of additives on the melting point," *J. Sol. Energy Eng. Trans. ASME*, vol. 134, no. 4, pp. 1–8, 2012, doi: 10.1115/1.4006895.

[18] H. Tian, L. Du, X. Wei, S. Deng, W. Wang, and J. Ding, "Enhanced thermal conductivity of ternary carbonate salt phase change material with Mg particles for solar thermal energy storage," *Appl. Energy*, vol. 204, pp. 525–530, 2017, doi: 10.1016/j.apenergy.2017.07.027.

[19] H. O. Pierson, *Handbook of Carbon, Graphite, Diamonds and Fullerenes: Processing, Properties and Aplications*. Noves Publications, 1994.

[20] Z. Ge, F. Ye, H. Cao, G. Leng, Y. Qin, and Y. Ding, "Carbonate-salt-based composite materials for medium- and high-temperature thermal energy storage," *Particuology*, vol. 15, pp. 77–81, 2014, doi: 10.1016/j.partic.2013.09.002.

[21] N. Navarrete, "Development of nanofluids based on nanoencapsulated phase change materials," Universitat Jaume I, Castelló de la Plana, 2020.

[22] A. Bonk, S. Sau, N. Uranga, M. Hernaiz, and T. Bauer, "Advanced heat transfer fluids for direct molten salt line-focusing CSP plants," *Prog. Energy Combust. Sci.*, vol. 67, pp. 69–87, 2018, doi: 10.1016/j.pecs.2018.02.002.

[23] R. Grena and P. Tarquini, "Solar linear Fresnel collector using molten nitrates as heat transfer fluid," *Energy*, vol. 36, no. 2, pp. 1048–1056, 2011, doi: 10.1016/j.energy.2010.12.003.

[24] D. Grogan, "Development of Molten Salt HTF technology for Parabolic Trough Solar Power Plants - Public Final Technical Report. DOE/08GO18038.," pp. 303–323, 2013.

[25] E. González-Roubaud, D. Pérez-Osorio, and C. Prieto, "Review of commercial thermal energy storage in concentrated solar power plants: Steam vs. molten salts," *Renew. Sustain. Energy Rev.*, vol. 80, no. May, pp. 133–148, 2017, doi: 10.1016/j.rser.2017.05.084.

[26] B. Kelly and D. Kearney, "Thermal Storage Commercial Plant Design Study for a 2-Tank Indirect Molten Salt System: Final Report; May 13, 2002 - December 31, 2004," no. July, 2002.

[27] T. Bauer, N. Pfleger, D. Laing, W. D. Steinmann, M. Eck, and S. Kaesche, *High-Temperature Molten Salts for Solar Power Application*. Elsevier Inc., 2013.

[28] R. G. Reddy, "Novel Molten Salts Thermal Energy Storage for Concentrating Solar Power Generation," Golden, CO (United States), Oct. 2013. doi: 10.2172/1111584.

[29] N. Pfleger, T. Bauer, C. Martin, M. Eck, and A. Wörner, "Thermal energy storage - overview and specific insight into nitrate salts for sensible and latent heat storage," *Beilstein J. Nanotechnol.*, vol. 6, no. 1, pp. 1487–1497, 2015, doi: 10.3762/bjnano.6.154.

[30] M. Mehos *et al.*, "Concentrating Solar Power Gen3 Demonstration Roadmap," *Nrel/Tp-*

5500-67464, no. January, pp. 1–140, 2017, doi: 10.2172/1338899.

[31] A. G. Fernández, J. Gomez-Vidal, E. Oró, A. Kruizenga, A. Solé, and L. F. Cabeza, "Mainstreaming commercial CSP systems: A technology review," *Renew. Energy*, vol. 140, pp. 152–176, Sep. 2019, doi: 10.1016/j.renene.2019.03.049.

[32] D. F. Williams, *Assessment of Candidate Molten Salt Coolants for the NGNP/NHI Heat-Transfer Loop*, no. March. 2006.

[33] D. E. Holcomb and S. M. Cetiner, *An Overview of Liquid-Fluoride-Salt Heat Transport Systems*, no. September. 2010.

[34] R. Serrano-ópez, J. Fradera, and S. Cuesta-López, "Molten salts database for energy applications," *Chem. Eng. Process. - Process Intensif.*, vol. 73, pp. 87–102, 2013, doi: 10.1016/j.cep.2013.07.008.

[35] D. F. Williams, L. M. Toth, and K. T. Clarno, *Assessment of Candidate Molten Salt Coolants for the Advanced High-Temperature Reactor (AHTR)*, no. March. 2006.

[36] G. Mohan, M. B. Venkataraman, and J. Coventry, "Sensible energy storage options for concentrating solar power plants operating above 600 °C," *Renew. Sustain. Energy Rev.*, vol. 107, no. November 2017, pp. 319–337, 2019, doi: 10.1016/j.rser.2019.01.062.

[37] H. Masuda, A. Ebata, K. Teramae, and N. Hishinuma, "Alteration of Thermal Conductivity and Viscosity of Liquid by Dispersing Ultra-Fine Particles. Dispersion of Al2O3, SiO2 and TiO2 Ultra-Fine Particles.," *Netsu Bussei*, vol. 7, no. 4, pp. 227–233, 1993, doi: 10.2963/jjtp.7.227.

[38] S. U. S. Choi, "Enhancing thermal conductivity of fluids with nanoparticles," in *American Society of Mechanical Engineers, Fluids Engineering Division (Publication) FED*, 1995, vol. 231, pp. 99–105.

[39] D. Shin and D. Banerjee, "Experimental Investigation of Molten Salt Nanofluid for Solar Thermal Energy Application," in *ASME/JSME 2011 8th Thermal Engineering Joint Conference*, Jan. 2011, pp. T30024-T30024-6, doi: 10.1115/AJTEC2011-44375.

[40] D. Shin and D. Banerjee, "Enhancement of specific heat capacity of high-temperature silica-nanofluids synthesized in alkali chloride salt eutectics for solar thermal-energy storage applications," *Int. J. Heat Mass Transf.*, vol. 54, no. 5–6, pp. 1064–1070, 2011, doi: 10.1016/j.ijheatmasstransfer.2010.11.017.

[41] S. F. Ahmed, M. Khalid, W. Rashmi, A. Chan, and K. Shahbaz, "Recent progress in solar thermal energy storage using nanomaterials," *Renew. Sustain. Energy Rev.*, vol. 67, pp. 450–460, 2017, doi: 10.1016/j.rser.2016.09.034.

[42] G. Qiao, M. Lasfargues, A. Alexiadis, and Y. Ding, "Simulation and experimental study of the specific heat capacity of molten salt based nanofluids," *Appl. Therm. Eng.*, vol. 111, pp. 1517–1522, 2016, doi: 10.1016/j.applthermaleng.2016.07.159.

[43] L. Wang, Z. Tan, S. Meng, D. Liang, and G. Li, "Enhancement of molar heat capacity of nanostructured Al2O3," *J. Nanoparticle Res.*, vol. 3, no. 5–6, pp. 483–487, 2001, doi: 10.1023/A:1012514216429.

[44] L. Xue, P. Keblinski, S. R. Phillpot, S. U. S. Choi, and J. A. Eastman, "Effect of liquid layering at the liquid-solid interface on thermal transport," *Int. J. Heat Mass Transf.*, vol. 47, no. 19–20, pp. 4277–4284, 2004, doi: 10.1016/j.ijheatmasstransfer.2004.05.016.

[45] L. Li, Y. Zhang, H. Ma, and M. Yang, "Molecular dynamics simulation of effect of liquid

layering around the nanoparticle on the enhanced thermal conductivity of nanofluids," *J. Nanoparticle Res.*, vol. 12, no. 3, pp. 811–821, 2010, doi: 10.1007/s11051-009-9728-5.

[46] A. Svobodova-Sedlackova, C. Barreneche, G. Alonso, A. I. Fernandez, and P. Gamallo, "Effect of nanoparticles in molten salts – MD simulations and experimental study," *Renew. Energy*, vol. 152, pp. 208–216, 2020, doi: 10.1016/j.renene.2020.01.046.

[47] R. Mondragón, J. E. Juliá, L. Cabedo, and N. Navarrete, "On the relationship between the specific heat enhancement of salt-based nanofluids and the ionic exchange capacity of nanoparticles," *Sci. Rep.*, vol. 8, no. 1, pp. 1–12, 2018, doi: 10.1038/s41598-018-25945-0.

[48] S. M. M. Rizvi and D. Shin, "Mechanism of heat capacity enhancement in molten salt nanofluids," *Int. J. Heat Mass Transf.*, vol. 161, p. 120260, Nov. 2020, doi: 10.1016/j.ijheatmasstransfer.2020.120260.

[49] H. Riazi, T. Murphy, G. B. Webber, R. Atkin, S. S. M. Tehrani, and R. A. Taylor, "Specific heat control of nanofluids: A critical review," *Int. J. Therm. Sci.*, vol. 107, pp. 25–38, 2016, doi: 10.1016/j.ijthermalsci.2016.03.024.

[50] O. Arthur and M. A. Karim, "An investigation into the thermophysical and rheological properties of nanofluids for solar thermal applications," *Renew. Sustain. Energy Rev.*, vol. 55, pp. 739–755, Mar. 2016, doi: 10.1016/j.rser.2015.10.065.

[51] B. Muñoz-Sánchez, J. Nieto-Maestre, I. Iparraguirre-Torres, A. García-Romero, and J. M. Sala-Lizarraga, "Molten salt-based nanofluids as efficient heat transfer and storage materials at high temperatures. An overview of the literature," *Renew. Sustain. Energy Rev.*, vol. 82, no. February 2017, pp. 3924–3945, 2018, doi: 10.1016/j.rser.2017.10.080.

[52] V. M. B. Nunes, M. J. V. Lourenço, F. J. V. Santos, and C. A. Nieto de Castro, "Molten alkali carbonates as alternative engineering fluids for high temperature applications," *Appl. Energy*, vol. 242, pp. 1626–1633, May 2019, doi: 10.1016/j.apenergy.2019.03.190.

[53] D. Ercole, O. Manca, and K. Vafai, "An investigation of thermal characteristics of eutectic molten salt-based nano fl uids," *Int. Commun. Heat Mass Transf.*, vol. 87, pp. 98–104, 2017, doi: 10.1016/j.icheatmasstransfer.2017.06.022.

[54] G. J. Janz and M. R. Lorenz, "Solid-Liquid Phase Equilibria for Mixtures of Lithium, Sodium, and Potassium Carbonates," *J. Chem. Eng. Data*, vol. 6, no. 3, pp. 321–323, Jul. 1961, doi: 10.1021/je00103a001.

[55] N. Araki, M. Matsuura, A. Makino, T. Hirata, and Y. Kato, "Measurement of thermophysical properties of molten salts: Mixtures of alkaline carbonate salts," *Int. J. Thermophys.*, vol. 9, no. 6, pp. 1071–1080, 1988, doi: 10.1007/BF01133274.

[56] FactSage, "K2CO3-Li2CO3 Binary Phase Diagram." .

[57] B. Jo and D. Banerjee, "Thermal properties measurement of binary carbonate salt mixtures for concentrating solar power plants," *J. Renew. Sustain. Energy*, vol. 7, no. 3, p. 033121, May 2015, doi: 10.1063/1.4922029.

[58] P. L. Spedding, "Densities and Molar Volumes of Molten Alkali Carbonate Binary Mixtures," *J. Electrochem. Soc.*, vol. 117, no. 2, p. 177, 1970, doi: 10.1149/1.2407460.

[59] G. J. Janz, C. B. Allen, N. P. Bansal, R. M. Murphy, and R. P. T. Tomkins, "Physical Properties Data Compilations Relevant To Energy Storage - 2. Molten Salts: Data on Single and Multi-Component Salt Systems.," *Natl. Bur. Stand. Natl. Stand. Ref. Data Ser.*, no. 61 pt 2, 1979.

[60] L. G. Marianowski and H. C. Maru, “Latent heat thermal energy storage systems above 450 C,” in *Intersociety Energy Conversion Engineering Conference, 12th. Proceedings.*, 1977, pp. 555–566.

[61] H. C. Maru *et al.*, “MOLTEN SALT THERMAL ENERGY STORAGE SYSTEMS.,” 1978.

[62] T. Kojima, Y. Miyazaki, K. Nomura, and K. Tanimoto, “ Physical Properties of Molten Li 2 CO 3 -Na 2 CO 3 (52:48 mol%) and Li 2 CO 3 -K 2 CO 3 (62:38 mol%) Containing Additives ,” *J. Electrochem. Soc.*, vol. 160, no. 10, pp. H733–H741, 2013, doi: 10.1149/2.073410jes.

[63] D. Shin, “Molten salt nanomaterials for thermal energy storage and concentrated solar power applications,” 2011.

[64] D. Shin and D. Banerjee, “Enhanced thermal properties of SiO2 nanocomposite for solar thermal energy storage applications,” *Int. J. Heat Mass Transf.*, vol. 84, pp. 898–902, 2015, doi: 10.1016/j.ijheatmasstransfer.2015.01.100.

[65] Y. B. Tao, C. H. Lin, and Y. L. He, “Preparation and thermal properties characterization of carbonate salt/carbon nanomaterial composite phase change material,” *Energy Convers. Manag.*, vol. 97, pp. 103–110, 2015, doi: 10.1016/j.enconman.2015.03.051.

[66] G. J. Janz and F. Saegusa, “Molten Carbonates as Electrolytes: Viscosity and Transport Properties,” *J. Electrochem. Soc.*, vol. 110, no. 5, p. 452, 1963, doi: 10.1149/1.2425785.

[67] Y. Sato *et al.*, “Viscosities of Molten Alkali Carbonates.,” *Netsu Bussei*, vol. 13, no. 3. pp. 156–161, 1999, doi: 10.2963/jjtp.13.156.

[68] D. Di Genova, C. Cimarelli, K. U. Hess, and D. B. Dingwell, “An advanced rotational rheometer system for extremely fluid liquids up to 1273 K and applications to alkali carbonate melts,” *Am. Mineral.*, vol. 101, no. 4, pp. 953–959, 2016, doi: 10.2138/am-2016-5537CCBYNCND.

[69] S. V. Vorob’ev, G.V., Pal’guev, S.F., and Karpachev, *Electrochemistry of Molten and Solid Electrolytes, Vol. 3*, No. 6. New York: Consultants Bureau, 1966.

[70] Y. Sato, T. Yamazaki, H. Kato, H. Zhu, M. Hoshi, and T. Yamamura, “Viscosities of Li2CO3-Na2CO3 and Li2CO3-K2CO3 Binary Melts.,” *Netsu Bussei*, vol. 13, no. 3. pp. 162–167, 1999, doi: 10.2963/jjtp.13.162.

[71] S. Lee, M. Kim, M. Hwang, K. Kim, C. Jeon, and J. Song, “Thermal stability and viscosity behaviors of hot molten carbonate mixtures,” *Exp. Therm. Fluid Sci.*, vol. 49, pp. 94–104, 2013, doi: 10.1016/j.expthermflusci.2013.04.006.

[72] S. W. Kim, K. Uematsu, K. Toda, and M. Sato, “Viscosity analysis of alkali metal carbonate molten salts at high temperature,” *J. Ceram. Soc. Japan*, vol. 123, no. 1437, pp. 355–358, 2015, doi: 10.2109/jcersj2.123.355.

[73] B. Jo and D. Banerjee, “Viscosity measurements of multi-walled carbon nanotubes-based high temperature nanofluids,” *Mater. Lett.*, vol. 122, pp. 212–215, May 2014, doi: 10.1016/j.matlet.2014.02.032.

[74] B. El Far, S. M. M. Rizvi, Y. Nayfeh, and D. Shin, “Investigation of heat capacity and viscosity enhancements of binary carbonate salt mixture with SiO2 nanoparticles,” *Int. J. Heat Mass Transf.*, vol. 156, pp. 1–5, 2020, doi: 10.1016/j.ijheatmasstransfer.2020.119789.

[75] M. M. Kenisarin, “High-temperature phase change materials for thermal energy storage,” *Renew. Sustain. Energy Rev.*, vol. 14, no. 3, pp. 955–970, Apr. 2010, doi:

10.1016/j.rser.2009.11.011.

[76] X. Zhang and M. Fujii, “Simultaneous measurements of the thermal conductivity and thermal diffusivity of molten salts with a transient short-hot-wire method,” *Int. J. Thermophys.*, vol. 21, no. 1, pp. 71–84, 2000, doi: 10.1023/A:1006604820755.

[77] M. A. Geyer, “Thermal Storage for Solar Power Plants,” *Sol. Power Plants*, pp. 199–214, 1991, doi: 10.1007/978-3-642-61245-9_6.

[78] Y. Shiina and T. Inagaki, “Study on the efficiency of effective thermal conductivities on melting characteristics of latent heat storage capsules,” *Int. J. Heat Mass Transf.*, vol. 48, no. 2, pp. 373–383, Jan. 2005, doi: 10.1016/j.ijheatmasstransfer.2004.07.043.

[79] G. J. Janz, E. Neuenschwander, and F. J. Kelly, “High-temperature heat content and related properties for Li2CO3, Na2CO3, K2CO3, and the ternary eutectic mixture,” *Trans. Faraday Soc.*, vol. 59, p. 841, 1963, doi: 10.1039/tf9635900841.

[80] G. J. Janz and J. L. Perano, “High-temperature heat content and fusion properties for binary carbonate mixtures: Li2CO3, K2CO3 and Na2CO3,” *Trans. Faraday Soc.*, vol. 60, p. 1742, 1964, doi: 10.1039/tf9646001742.

[81] M. Liu, J. C. Gomez, C. S. Turchi, N. H. S. Tay, W. Saman, and F. Bruno, “Determination of thermo-physical properties and stability testing of high-temperature phase-change materials for CSP applications,” *Sol. Energy Mater. Sol. Cells*, vol. 139, pp. 81–87, 2015, doi: 10.1016/j.solmat.2015.03.014.

[82] B. Jo and D. Banerjee, “Effect of solvent on specific heat capacity enhancement of binary molten salt-based carbon nanotube nanomaterials for thermal energy storage,” *Int. J. Therm. Sci.*, vol. 98, pp. 219–227, 2015, doi: 10.1016/j.ijthermalsci.2015.07.020.

[83] H. Kim and B. Jo, “Anomalous Increase in Specific Heat of Binary Molten Salt-Based Graphite Nanofluids for Thermal Energy Storage,” *Appl. Sci.*, vol. 8, no. 8, p. 1305, 2018, doi: 10.3390/app8081305.

[84] J. R. Selman and H. C. Maru, “PHYSICAL CHEMISTRY AND ELECTROCHEMISTRY OF ALKALI CARBONATE MELTS WITH SPECIAL REFERENCE TO THE MOLTEN-CARBONATE FUEL CELL,” *Adv. Molten Salt Chem.*, vol. 4, no. 159–390, 1981.

[85] D. Shin and D. Banerjee, “Enhanced Specific Heat of Silica Nanofluid,” *J. Heat Transfer*, vol. 133, no. 2, pp. 23–26, Feb. 2011, doi: 10.1115/1.4002600.

[86] D. Shin and D. Banerjee, “Enhanced Specific Heat Capacity of Nanomaterials Synthesized by Dispersing Silica Nanoparticles in Eutectic Mixtures,” *J. Heat Transfer*, vol. 135, no. 3, p. 032801, Mar. 2013, doi: 10.1115/1.4005163.

[87] H. Tiznobaik and D. Shin, “Enhanced specific heat capacity of high-temperature molten salt-based nanofluids,” *Int. J. Heat Mass Transf.*, vol. 57, no. 2, pp. 542–548, 2013, doi: 10.1016/j.ijheatmasstransfer.2012.10.062.

[88] B. Jo and D. Banerjee, “Enhanced specific heat capacity of molten salt-based nanomaterials: Effects of nanoparticle dispersion and solvent material,” *Acta Mater.*, vol. 75, pp. 80–91, 2014, doi: 10.1016/j.actamat.2014.05.005.

[89] B. Jo and D. Banerjee, “Enhanced Specific Heat Capacity of Molten Salt-Based Carbon Nanotubes Nanomaterials,” *J. Heat Transfer*, vol. 137, no. 9, p. 091013, 2015, doi: 10.1115/1.4030226.

[90] H. Tiznobaik, D. Banerjee, and D. Shin, “Effect of formation of ‘long range’ secondary

dendritic nanostructures in molten salt nanofluids on the values of specific heat capacity," *Int. J. Heat Mass Transf.*, vol. 91, pp. 342–346, 2015, doi: 10.1016/j.ijheatmasstransfer.2015.05.072.

[91] L. Sang, W. Ai, T. Liu, Y. Wu, and C. Ma, "Insights into the specific heat capacity enhancement of ternary carbonate nanofluids with SiO 2 nanoparticles: the effect of change in the composition ratio," *RSC Adv.*, vol. 9, no. 10, pp. 5288–5294, 2019, doi: 10.1039/c8ra10318f.

[92] S. M. M. Rizvi, B. El Far, Y. Nayfeh, and D. Shin, "Investigation of time–temperature dependency of heat capacity enhancement in molten salt nanofluids," *RSC Adv.*, vol. 10, no. 39, pp. 22972–22982, 2020, doi: 10.1039/D0RA03666H.

[93] R. Hentschke, "On the specific heat capacity enhancement in nanofluids," *Nanoscale Res. Lett.*, vol. 11, no. 1, pp. 1–11, 2016, doi: 10.1186/s11671-015-1188-5.

[94] M. Chieruzzi, G. F. Cerritelli, A. Miliozzi, and J. M. Kenny, "Effect of nanoparticles on heat capacity of nanofluids based on molten salts as PCM for thermal energy storage," *Nanoscale Res. Lett.*, vol. 8, no. 1, pp. 1–9, 2013, doi: 10.1186/1556-276X-8-448.

[95] P. Andreu-Cabedo, R. Mondragon, L. Hernandez, R. Martinez-Cuenca, L. Cabedo, and J. E. Julia, "Increment of specific heat of Solar Salt with SiO2 and Al2O3 nanoparticles," *Nanoscale Res. Lett.*, vol. 9, no. 1, p. 582, 2014, doi: 10.1186/1556-276X-9-582.

[96] H. Tiznobaik and D. Shin, "Experimental validation of enhanced heat capacity of ionic liquid-based nanomaterial," *Appl. Phys. Lett.*, vol. 102, no. 17, p. 173906, Apr. 2013, doi: 10.1063/1.4801645.

[97] D. Shin and D. Banerjee, "Specific heat of nanofluids synthesized by dispersing alumina nanoparticles in alkali salt eutectic," *Int. J. Heat Mass Transf.*, vol. 74, pp. 210–214, 2014, doi: 10.1016/j.ijheatmasstransfer.2014.02.066.

[98] Y. Grosu *et al.*, "Solar Energy Materials and Solar Cells Nanofluids based on molten carbonate salts for high-temperature thermal energy storage : Thermophysical properties , stability , compatibility and life cycle analysis," vol. 220, no. April 2020, 2021, doi: 10.1016/j.solmat.2020.110838.

[99] Y. Grosu, U. Nithiyanantham, L. González-Fernández, and A. Faik, "Preparation and characterization of nanofluids based on molten salts with enhanced thermophysical properties for thermal energy storage at concentrate solar power," *AIP Conf. Proc.*, vol. 2126, 2019, doi: 10.1063/1.5117736.